Investigating the Phenotypical Effects of An Adaptable Multi-Modality pH-Sensitive Nanoprobe for Real-Time Monitoring of Engineered Cells and Tissues.

by

Albert Essuman

A Thesis Presented in Partial Fulfillment
of the Requirement for the Degree
Master of Science

Approved April 2021 by the
Graduate Supervisory Committee:

David Brafman, Chair
Jessica Weaver
Vikram Kodibagkar

ARIZONA STATE UNIVERSITY

May 2021

ABSTRACT

Cells and tissues play an important role in disease modelling, drug screening and in regenerative medicine applications. In the development and subsequent usage of cells and tissues, it is imperative that the viability of the construct is always assessed. According to BioFab USA and the National Cell Manufacturing Consortium, in-line monitoring of biomanufactured tissues is critical for downstream applications in disease modeling, drug screening and regenerative medicine. Intracellular pH of cells characterizes different activities of the cell including metabolism, proliferation, differentiation, and apoptosis and provide a great opportunity for the assessment of cell and tissue viability.

Current technologies have utilized fluorescence probes, MRI, PET and CT techniques to measure cellular pH and to determine cellular and tissue viability. The current technologies have been limited by several factors including the use of custom hardware and software, incompatibility with different culture systems, tissues, and cell types, and the inability to scale into the existing cell and tissue production process. Ratiometric probes for measuring and analyzing of pH has generated scientific interest recently as it provides an accurate measurement of pH independent of probe concentration or excitation energy. Previously, a team of scientist from Arizona State University collaborating with others developed an adaptable multimodality pH sensitive probe for non-invasive real-time monitoring of cells and tissues to solve the current problem.

In this study, the phenotypical effects of the pH probe were investigated using proliferative and non-proliferative cells in different culture systems. Specifically, the efficiency of the probes in labeling cells in 2D, microcarriers and Matrigel culture systems was determined. Proliferation of cells and cell phenotypes were not affected by labeling with the pH probe and pH dependency were demonstrated in all culture systems.

DEDICATION

I dedicate this thesis to…

My son, Leonard Essuman-Mintah Junior and my spouse Augustina

for the support, encouragement, and inspiration even in challenging times.

Thank you! Your endless love, sacrifice and prayers made this journey possible.

ACKNOWLEDGEMENTS

My sincerest gratitude first goes to Dr. David Brafman for giving me the opportunity to explore and build on my knowledge under his mentorship. I am extremely grateful for the support, patience, and guidance he provided despite my lack of experience in the field, and more especially the confidence he had in me.

I am also grateful to all Brafman Lab members for the support and willingness to answer all my questions during the execution of this project. I am especially thankful to Jacob Knittel for teaching me all the lab practices and skills necessary for the execution of this work.

Special thanks to my committee members, Dr. Jessica Weaver and Dr. Vikram Kodibagkar for all their inputs and guidance. Thank you for the time to review my data and for providing relevant inputs that made the completion of this thesis possible.

TABLE OF CONTENTS

Page

CHAPTER Page

LIST OF FIGURES

Figure Page

LIST OF ABBREVIATIONS

2D	Two dimensional
3D	Three dimensional
ASD	Autism spectrum disorders
BDNF	Brain-derived neurotrophic factor
CT	Computed tomography
EGF	Epidermal growth factor
ER	Endoplasmic reticulum
FGF	Fibroblast growth factor
FMR1	Fragile X mental retardation gene
GDNF	Glia cell-derived neurotrophic factor
HESC	Human embryonic stem cells
hiPSC	Human induced pluripotent stem cell
HNPC	Human neural progenitor cells
MC	Microcarrier
MRI	Magnetic resonance imaging
NBM	Neural base media
NDM	Neural differentiation media
NEM	Neural expansion media
NPC	Neural progenitor cell
PBS	Phosphate-buffered saline
PCR	Polymerase chain reaction
PET	Positron emission tomography
SMA	Spinal muscular atrophy

1 INTRODUCTION

1.1 Stem Cells and Cell Viability

There has been increasing use of cells, particularly stem cells in the field of tissue engineering due to their ability to differentiate into different cell types in the body. Stems cells are basic cells that can differentiate into different cell types in the body and have provided a great avenue for accurate modelling of several human diseases and for drug development. Stem cells have been used in the modelling of simple human disease and other much more complex diseases[1]. Fragile X syndrome, a relatively simple genetic disease that results from the inactivation of the FMR1 gene has been successfully modelled with the use of human embryonic stem cells (HESC) which have helped in uncovering the sequences by which the epigenetic change is acquired[2]. The FMR1 gene is an important gene that provides the instructions to produce FMRP protein present in the brain, ovaries and testes for normal cognitive functions and female reproductions. Stem cells have not only been used in the modelling of simple monogenic diseases like Fragile X syndrome alone, but also in more complex diseases such as schizophrenia[3] and autism spectrum disorders (ASD)[4].

Stems cells have also been successfully used in drug screening for the easy identification of drug candidates for numerous diseases. Utilizing RNA sequencing, motor neurons from spinal muscular atrophy (SMA) patients have been used to demonstrate hyper activation of the endoplasmic reticulum (ER) stress in SMA. This study showed that a systemic delivery of ER stress inhibitors that crosses the blood brain barrier led to the preservation of spinal cord motor neurons[5]. Several other works have used stem cell platforms to identify important molecules and pathways relevant for drug development in various diseases affecting humans[6] [7] [8].

With these increasing use of cells in disease modelling, drug screening, and other regenerative applications, it's imperative that the health and state of the cells is continuously monitored. Cell viability assays involve the process of determining the number of healthy cells in a cell based assay [9]. Knowing how viable the cells being used are will not only help to improve the accuracy of the results of experiments but also improve efficacy of treatments offered to patients.

1.2 Cellular pH and Cell Activities

The extracellular and intracellular pH of cells have great influence on the activities of the cells and gives important cues pertaining to the fate of the cell. Several activities of the cell have been linked to increasing intracellular pH or alkalinization including proliferation, glycolysis and protein synthesis[10]. There have also been several reports that have associated apoptosis to decreasing intracellular pH[11]. In tumor cells, there is an increasing rate of glucose catabolism which leads to high levels of lactate and hydrogen ions. As a result, an acidic extracellular pH has been reported as a key marker in tumor cells[12].

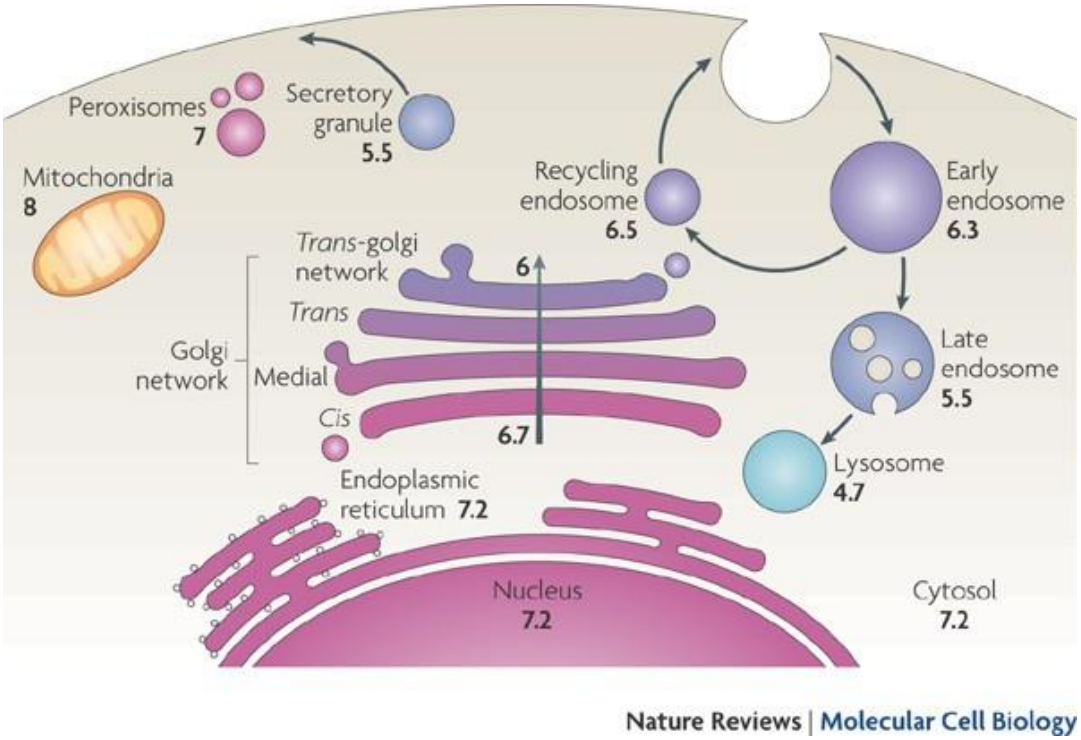

Figure 1: Heterogeneity of intracellular pH [13]

Intracellular pH of the cell is heterogenous with varying pHs from one organelle to the other as shown in the figure 1 above[13]. The average intracellular pH is regulated within narrow variation in animal cells at around 7.4[10]. Many cell activities are dependent on intracellular pH as reported above. Abnormal intracellular pH has been reported as the hallmark of several diseases including stroke, cancer, and Alzheimer's, it is therefore important to have an accurate and precise method for cellular pH measurement without causing any harm or phenotypical changes to the cell.

1.3 Current Research on Cellular pH Measurement

The pH of cells serves as a property that characterizes several activities and states of the cell. Intracellular pH has been reported to regulate very important activities of the cell including cellular metabolism, calcium signaling and cell migration[13].The differentiation and proliferation of stem cells has have also been demonstrated in several studies to be regulated by intracellular pH [15] [16]. The relevance of the information revealed by the pH of the cell has spiked the interest of many researchers to develop various techniques to measure cellular pH.

Fluorescent probes have been widely utilized as a mode for pH measurements as it provides a noninvasive means for measuring pH. Fluorescent probes also have higher resolutions compared to other techniques such as magnetic resonance imaging [17]. Previously, Zhang et al developed a fluorescence-based acidic pH sensitive probe utilizing rhodamine dyes and demonstrated its functionality using Human liver cancer cell line (HEPG2) [18]. Multimodal techniques for probe development that combines fluorescence with magnetic resonance imaging (MRI) or positron emission tomography(PET) with MRI or PET with computed tomography (CT) and several other possible combinations have been developed [19] [20] [21].

Ratiometric techniques for pH measurement have also been previously demonstrated based on MRI [22]. This technique helps to eradicate the influence of probe concentration and excitation energies on the measured pH values thereby increasing the accuracy of measurement [23]. Regardless of the promise and accuracy of the ratiometric technique, there have not been any ratiometric probe developed for cellular pH measurement [17]. Most of the intracellular pH probes that have been developed have been reported to have issues with cell permeability and cytotoxicity which have limited their usage [24]. The challenges faced by the current systems lead to the development of an adaptive multimodal pH sensitive nanoprobe for cellular pH measurements.

1.4 The Ratiometric pH Probe

In line with efforts to develop a more reliable technique for cellular pH sensing, Su et al developed a multifunctional polymer for ratiometric pH sensing, fluorescence imaging and magnetic resonance imaging[17]. The team utilized a gadolinium DOTA-based complex for MRI sensing synthesized as shown in figure 2 with the detailed preparation steps presented in the article[17]. The pH sensing component was integrated by using a previously developed probe as presented by Zhou et al [25]. Poly(2-(methacryloyloxy)ethyl]trimethylammonium chloride) (PTMAEOMA) which has been previously used as a cell permeable component for other fluorescence probes[26] [27] was added to improve cell permeability of the probe. Poly(*N*-2-hydroxypropyl methacrylamide) (PHPMA) which is widely known to be biocompatible and has been previously used in bioimaging[28] was also added to improve the biocompatibility of the probe. The complete pH/MRI probe was synthesized as shown in figure 2 and described in details in the article [17].

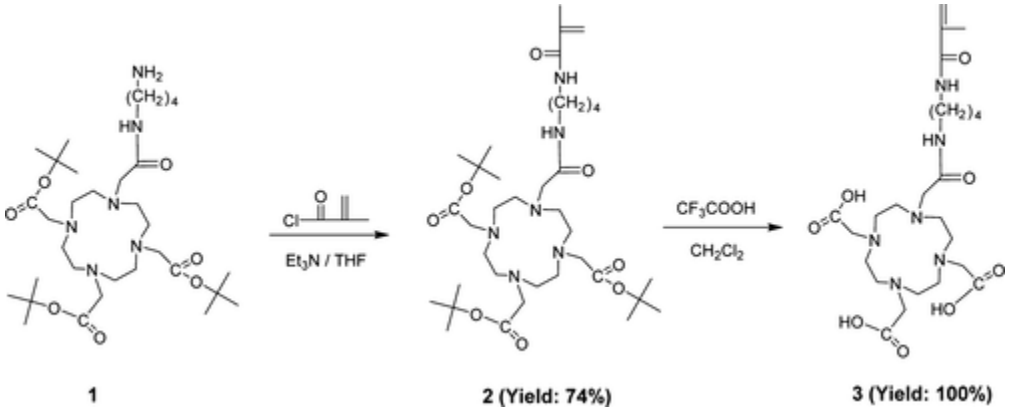

Figure 2: Synthesis of polymerizable MRI probe ligand 3

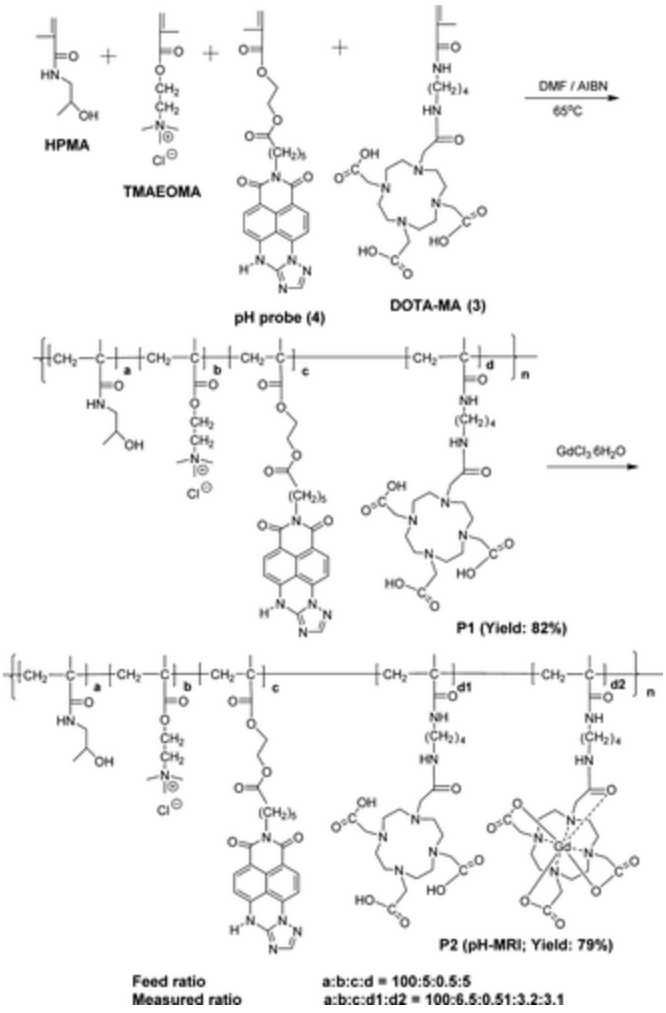

Figure 3: Synthesis of the dual modality ratiometric pH sensor of P2

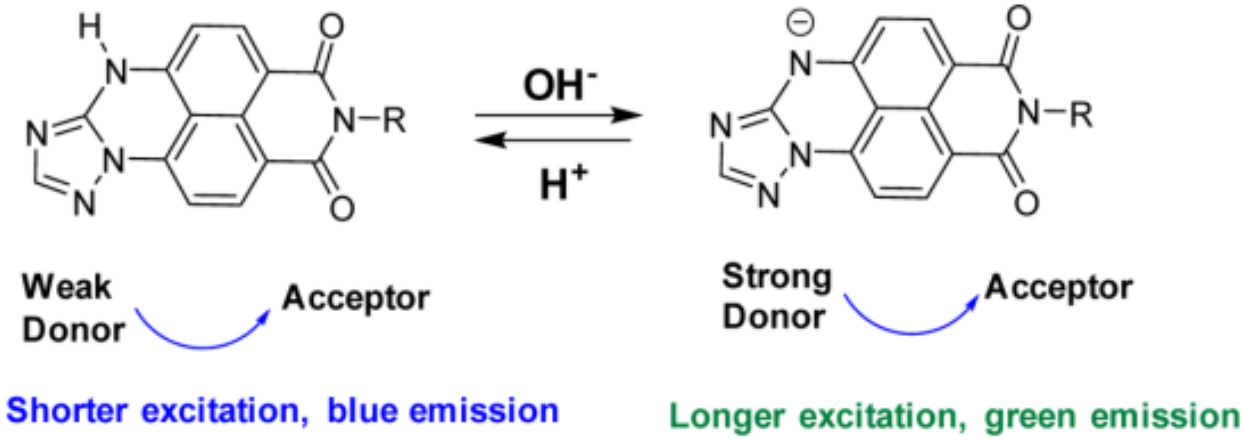

Figure 4; Drawing of the acid/base reaction of the pH dependent conjugate of the pH probe.

The chemistry of the pH dependent conjugate of the fluorescent probe as shown in figure 4 causes it to fluoresce high blue intensities in acidic conditions and high green intensities in basic conditions. Basically, under acidic conditions, the triazole unit is a relatively weak electron-donating group, whereas under basic conditions, the NH group at the triazole moiety is deprotonated to result in a stronger electron-donating ability of the triazole unit. Because of the electron-donating ability difference, the intramolecular charge transfer ability is affected by pH. The fluorescent intensity of the probe varies with changing pH and fluoresces bluer in acidic conditions and greener in basic conditions.

In the study where this probe was developed, the ratiometric intensities green/blue was demonstrated to be pH dependent figure 5a. The level of toxicity of the probe to cells was also studied using mouse macrophage J774.1A and the results showed no obvious cytotoxicity between the labeled and unlabeled control. In this study, we sought to investigate the performance of the probe in industrially applicable culture systems. Specifically, we will be investigating the labeling efficiency, pH dependency and phenotypic effects of the probe on cells in 2D, microcarrier and 3D Matrigel culture systems.

a.

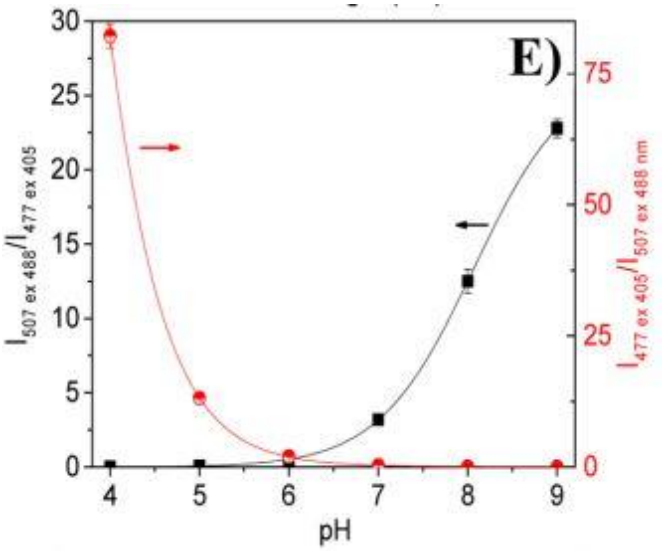

b.

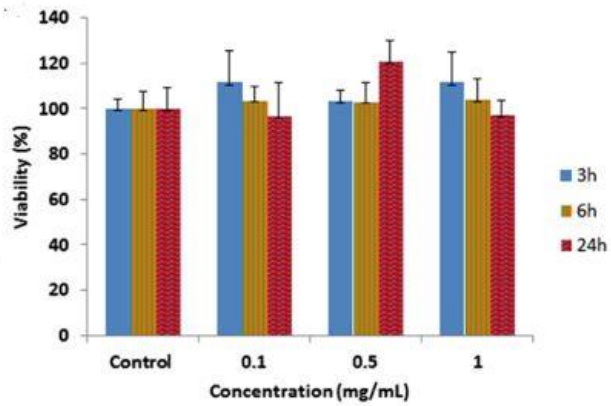

Figure 5; (a) Ratiometric pH dependency of the probe. (b) Cytotoxicity studies of the probe in mouse macrophage cells

1.5 Specific Aims of The Thesis

The objective of the thesis was to investigate the performance of the ratiometric pH sensitive probe previously developed by Su et al [17] in different culture systems and its effects on cellular phenotype. Specifically, the probe was studied in 2D, Microcarrier, and Matrigel culture systems using human neural progenitor cells and neurons.

Firstly, the labeling efficiency of the probe was investigated by culturing neurons and hNPCs in the different culture systems. For both neurons and hNPCs, microscopy-based or flow cytometry-based pH dependency were performed from the fluorescence intensity signals received from the cells post labeling with different concentrations of the probe. The number of cells dead or alive were measured and the percentage of cells labeled were quantified with flow cytometry for all culture systems.

Secondly, we investigated the pH dependency of the probes by tuning the intracellular pH of the cells and measuring the fluorescent intensities at different pH values for all culture systems. As the pH probe fluoresces bluer under acidic conditions and greener under basic conditions, we correlated pH values with the ratio of green/blue intensities.

Finally, cells were characterized post labeling to determine if the probe changes the phenotype of the cells. We started with proliferation studies using thawed hNPCs to ensure the cells retain their proliferative abilities post labeling. Immunofluorescence and quantitative PCR were performed to determine specific markers associated with the cells. For neurons, since calcium transient activities serve as a great characterizing mechanism, we performed calcium imaging analysis for all neurons in the different culture systems.

2 MATERIALS AND METHODS

2.1 Cell Culture

2.1.1 Media Preparation

Neural base media (NBM) were prepared by adding glutaMAX supplement, B-27 supplement, Penicillin-Streptomycin and N2 supplement to 500ml of DMEM/F12. Neural expansion media (NEM) were prepared by adding human epidermal growth factor (EGF) and fibroblast growth factor (FGF) to NBM. Human recombinant brain-derived neurotrophic factor (BDNF) and human recombinant glial cell-derived neurotrophic factor (GDNF) were added to NBM to make neural differentiation media.

2.1.2 2D hNPC

hNPCs were thawed and cultured on 10-centimeter plates at a seeding density of 600000 per well post thaw and 500000 for every subsequent passage. hNPCs were maintained in neural expansion media prepared as described in section **3.1.1** above. Media were changed every 24 hours and cells were cultured under standard conditions of 37 C, 5% CO2 and passaged at 70- 80% confluency.

2.1.3 2D Neurons

Matrigel solution with final concentration of 0.8% v/v is prepared by adding 200ul of stock matrigel (from R&D systems, catalog Number: 3433-010-01) aliquot to 25ml of DMEM 1X. Cell culture plates were coated with the matrigel solution and incubated at 37C for at least 30 minutes prior to neuron culture. Neurons were cultured in NBM on the matrigel coated plates and media were changed every 24 hours for seven days before being used for any experiment.

2.1.4 Microcarrier (MC) hNPC

Microcarriers were coated in poly-L-Ornithine (PLO) and laminin prior to cell culture. hNPC cells were maintained in culture for two passages post thaw and were seeded with the microcarriers at a seeding density of 1 million cells per well of a 6-well cell repellent plate in NEM with rock inhibitor. The culture was kept on static in an incubator for 12 hours and additional media and rock inhibitor were added and transferred to a shaker at 95 rpm. Microcarrier cultured cells were kept for a day before used for experiments.

2.1.5 Microcarrier Neurons

hNPCs were seeded on microcarriers as described in section **2.1.4.** Cells were maintained in NEM for 3 days with half media changes daily. On day 3 on NEM, a full media exchanged with NDM was done. The day of NDM switch was recognized as day 0 and half media exchange of NDM were conducted till day 17 of NDM. Full media exchange with NBM were conducted on day 18 and half media exchange with NBM was continued till day 30. Neurons were labeled on day 30 and used as aggregates or dissociated using a papain dissociation system protocol (previously developed by a group at Worthington Biochemical Corporation) [29] for various assays.

2.1.6 Matrigel hNPC and Neurons

Cells were cultured with a final Matrigel (from VWR) concentration of 5mg/ml for both hNPCs and neurons. Cells were seeded on a 24 well Matek plate (purchased from VWR) with total cell plus media plus matrigel of 200ul. The culture was kept on static in an incubator at 37 degrees for 90 minutes and 300ul additional media was added onto the culture, rock inhibitor is included in the case of hNPCs. Neurons are kept in culture for at least 7 days before use for any assays, hNPCs were used for assays from day 1 post culture.

2.1.7 Intracellular pH Tuning

Intracellular pH calibration kit (Thermo Fisher Scientific) was used to adjust the pH of cells for pH dependency test. Cells were maintained in the different culture systems and labeled with the pH probe. 24 hrs post labeling, the media and pH probe were washed and dissociated into single cells (for flow cytometry). The series of pH from the buffer kits (4.5, 5.5, 6.5, 7.5) were added and imaged using confocal microscope or flow cytometry was performed on the dissociated cells.

2.2 Labelling Efficiency and pH Dependency

2.2.1 pH Dependency – Flow Cytometry

Labeled cells were isolated from the culture system to ensure a single cell suspension. The cells were buffered to pH 4.5, 5.5, 6.5, and 7.5 with an intracellular pH calibration kit (Life Technologies P35379) for 15 minutes on ice. PI was added to the cell suspension 1 minute prior to analysis to assess cell viability. Cells were analyzed via flow cytometry using the Attune NxT (ThermoFisher) while still in the buffer solution. Data was analyzed with FlowJo. Median fluorescent intensity was quantified for the green and blue channel of live cells.

2.2.2 pH Dependency – Microscopy

Labeled cells in culture were subjected to intracellular pH calibration (Life Technologies P35379) for 5 minutes at 37C. While still in culture, cells were imaged with a Nikon Ti-Eclipse inverted microscope using an LED-based Lumencor SOLA SE Light Engine with a Semrock band pass filter. Cells in the MTGL culture system were imaged on a Leica TCS SP8 LSCM (NIH SIG award 1 S10 OD023691-01). Intensity of the images were determined with a MATLAB algorithm that excludes background intensities.

2.3 Cell Proliferation

hNPCs were cultured under standard conditions on 2D and on microcarriers. Triplicates of labeled and unlabeled cells were maintained in culture and passaged at 70-80 confluency for two consecutive passages. Labeled and unlabeled cells were counted after every passage with a hemocytometer. For the matrigel culture system, cells were cultured with triplicates of labeled and unlabeled cells and were passaged and counted after 48 hours post seeding.

2.4 Cell Characterization Assays

2.4.1 Immunofluorescence

Thawed neurons and hNPCs were cultured on 2D under standard conditions as describe in **section []**. Cells were washed twice with PBS prior to fixation. Cells were fixed with cytofix fixation buffer

(from BD Biosciences) and incubated at 4C for 20 minutes. The cells were then washed twice with PBS and permed with BD Phosflow Perm Buffer III (BD Biosciences) and incubated at room temperature for 30 minutes. The cells were washed twice after perming, stained with primary antibody, and incubated at 4C overnight. The cells were again washed twice and stained with secondary antibody for 1 hour at RT. The cells were washed twice after the hour incubation and DNA was stained with Hoechst dye for 10 minutes at RT. The cells were finally washed twice, PBS was added to the samples and imaged on a Nikon Eclipse Ti-2 microscope.

Microcarrier hNPCs were maintained in culture as described in **section [].** Cells were fixed in 15ml conicals and transferred to eppendolf tubes and the same staining protocol as the 2D culture was followed. After the Hoechst stain, slides were prepared from the samples using standard glass slide and a 1.5 thickness cover slip. The slides were images on a Leica SP5 confocal microscope.

Microcarrier neurons were dissociated from hNPCs after 30 days following the same method in **section.** The neurons were fixed, permed, stained, and imaged using the same method as was used in the 2D culture system. Matrigel neurons were cultured, dissociated, and following the same method as the 2D culture were fixed, permed, stained, and imaged.

2.5 Statistical Analysis

Ratiometric fluorescent intensity (green/blue) was enumerated and plotted against pH 4.5, 5.5, 6.5, 7.5 to produce a pH dependent curve for both flow cytometry and microscopy. Bio-triplicates were used to demonstrate reproducibility of ratiometric pH dependency. A simple linear regression yielded R sqared values and a one-way ANOVA showed a statistical significance between each pH value of the curve.

3 RESULTS

3.1 Labeling Efficiency and pH Dependency

3.1.1 2D Labeling Efficiency

a.

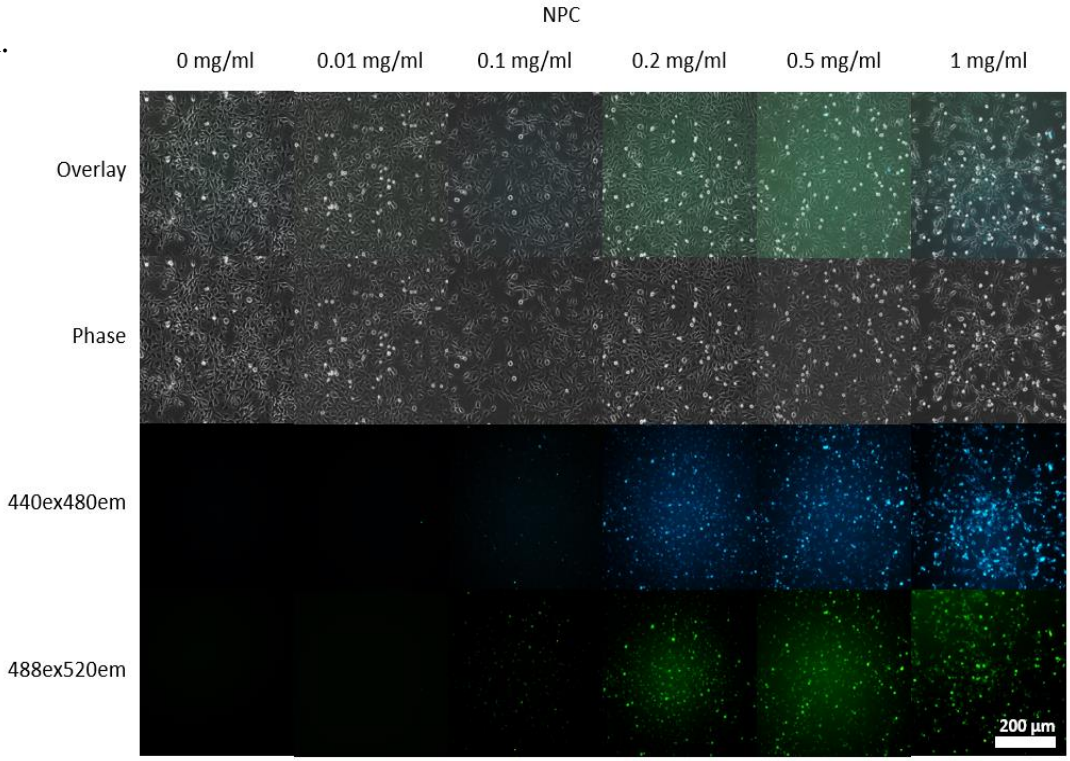

b.

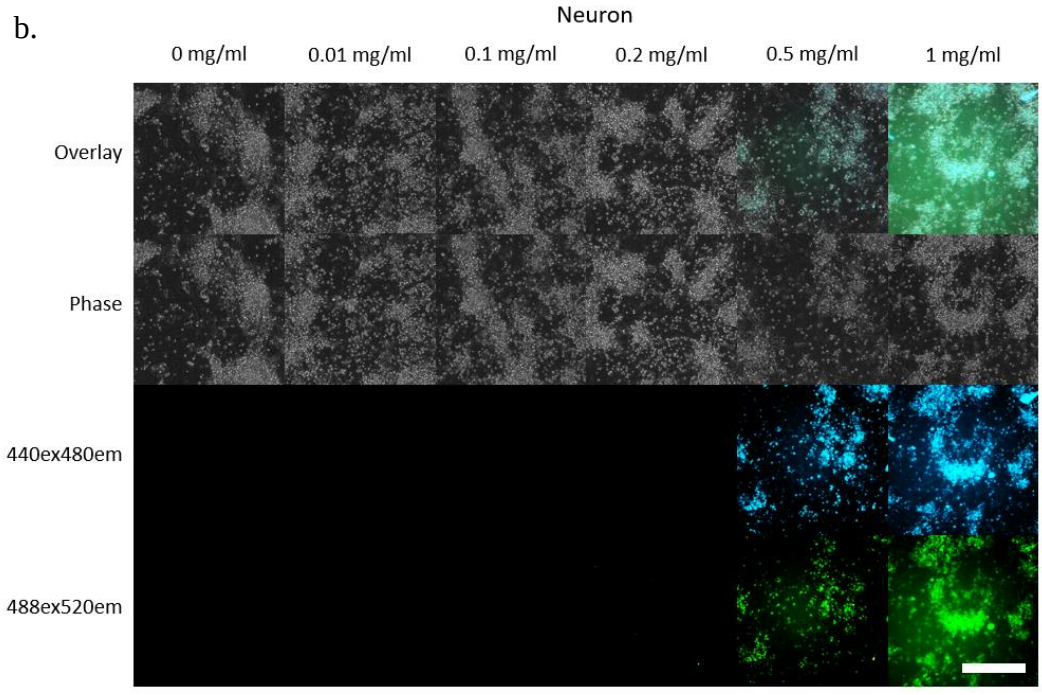

c.

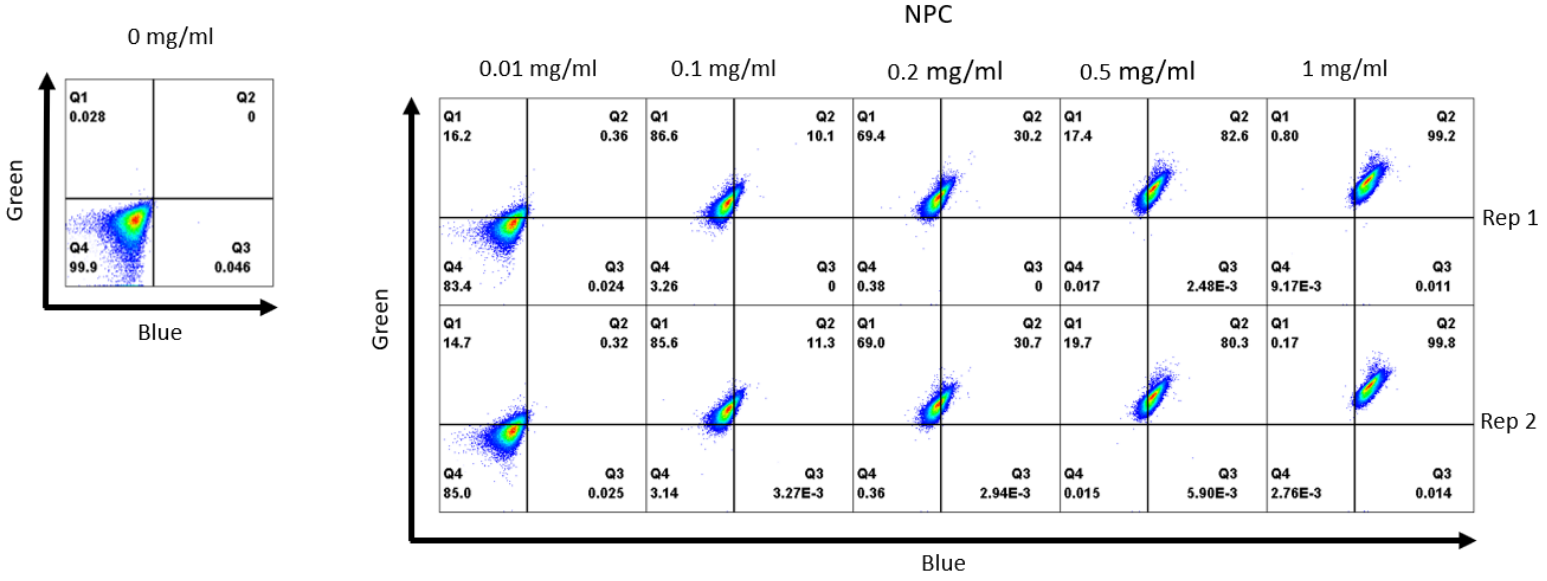
0 mg/ml
Q1 0.028
Q2 0
Q4 99.9
Q3 0.046
Green
Blue
NPC
0.01 mg/ml
0.1 mg/ml
0.2 mg/ml
0.5 mg/ml
1 mg/ml
Q1 16.2
Q2 0.36
Q4 83.4
Q3 0.024
Q1 86.6
Q2 10.1
Q4 3.26
Q3 0
Q1 69.4
Q2 30.2
Q4 0.38
Q3 0
Q1 17.4
Q2 82.6
Q4 0.017
Q3 2.48E-3
Q1 0.80
Q2 99.2
Q4 9.17E-3
Q3 0.011
Rep 1
Q1 14.7
Q2 0.32
Q4 85.0
Q3 0.025
Q1 85.6
Q2 11.3
Q4 3.14
Q3 3.27E-3
Q1 69.0
Q2 30.7
Q4 0.36
Q3 2.94E-3
Q1 19.7
Q2 80.3
Q4 0.015
Q3 5.90E-3
Q1 0.17
Q2 99.8
Q4 2.76E-3
Q3 0.014
Rep 2
Green
Blue

d.

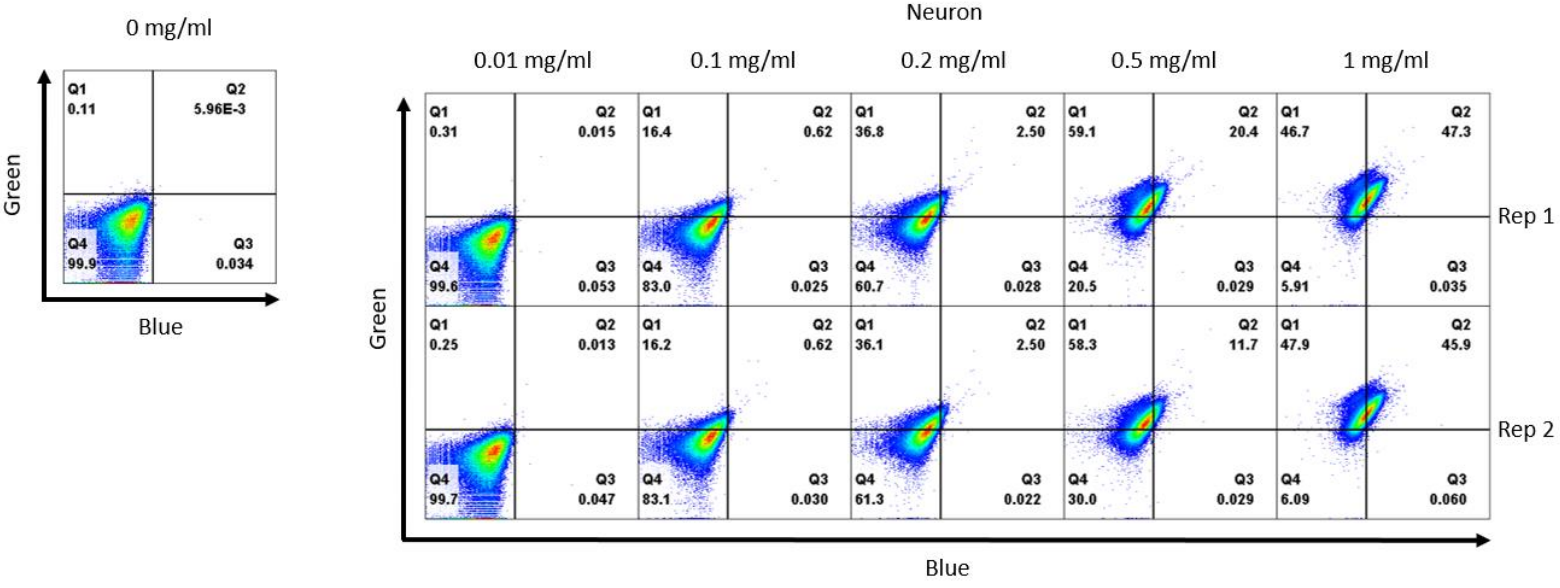
0 mg/ml
Q1 0.11
Q2 5.96E-3
Q4 99.9
Q3 0.034
Green
Blue
Neuron
0.01 mg/ml
0.1 mg/ml
0.2 mg/ml
0.5 mg/ml
1 mg/ml
Q1 0.31
Q2 0.015
Q4 99.6
Q3 0.053
Q1 16.4
Q2 0.62
Q4 83.0
Q3 0.025
Q1 36.8
Q2 2.50
Q4 60.7
Q3 0.028
Q1 59.1
Q2 20.4
Q4 20.5
Q3 0.029
Q1 46.7
Q2 47.3
Q4 5.91
Q3 0.035
Rep 1
Q1 0.25
Q2 0.013
Q4 99.7
Q3 0.047
Q1 16.2
Q2 0.62
Q4 83.1
Q3 0.030
Q1 36.1
Q2 2.50
Q4 61.3
Q3 0.022
Q1 58.3
Q2 11.7
Q4 30.0
Q3 0.029
Q1 47.9
Q2 45.9
Q4 6.09
Q3 0.060
Rep 2
Green
Blue

e.

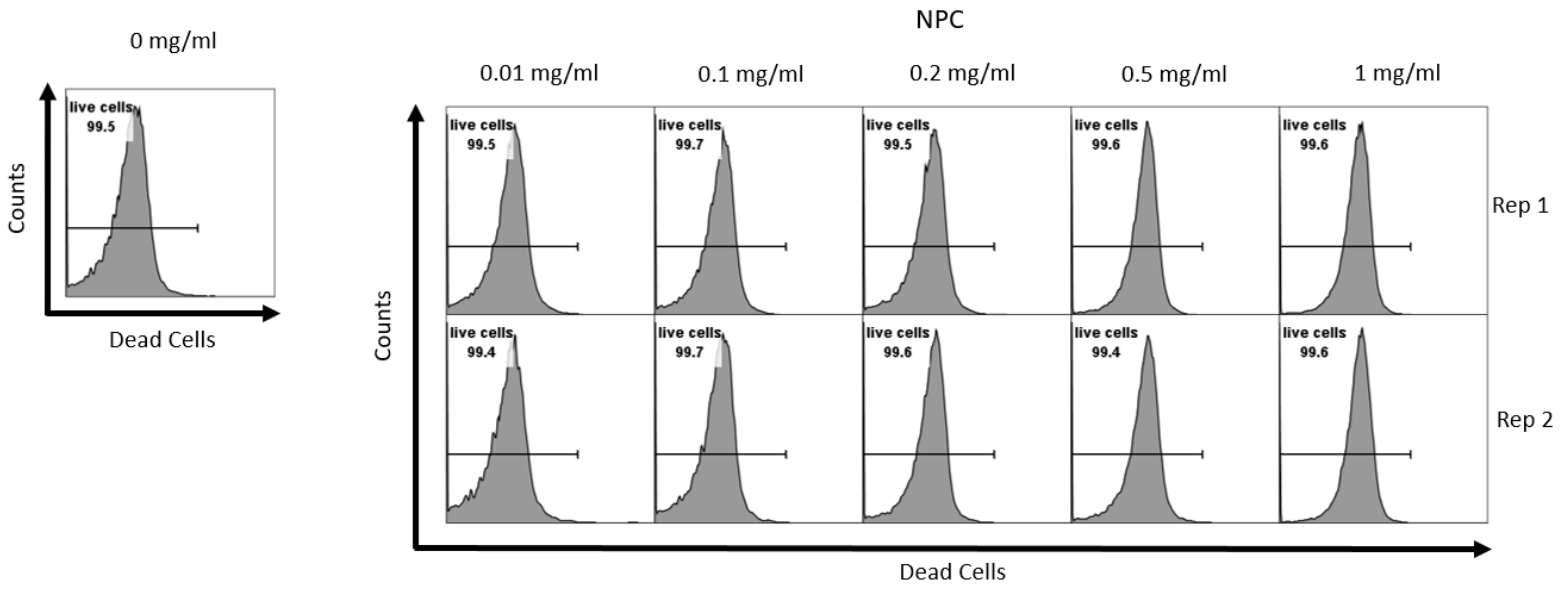

f.

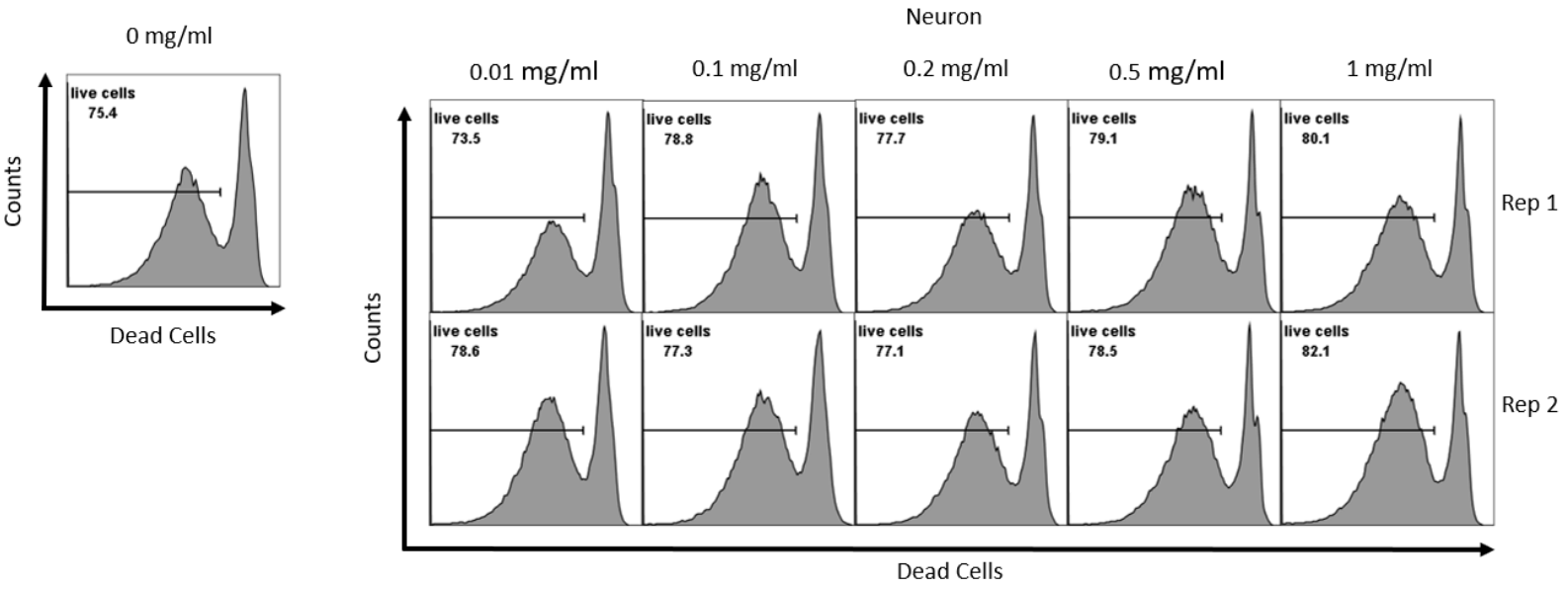

Figure 6: 2D Labeling Efficiency. a & b) Fluorescent images of hNPCs and neurons respectively from a confocal microscope with excitations for blue and green emission for different concentration of the probe. c& d) Flow plot showing labeling with green and blue emissions for hNPCs and neurons respectively for different values of probe concentration. e& f) Histogram showing dead and live cells for hNPCs and neurons respectively at the different labeling concentration.

The efficiency of the pH probe at labeling cells was previously demonstrated [17], nonetheless, these studies were performed with different cells and under different culture conditions compared to what we are utilizing in this project. We therefore investigated the efficiency of the probes in labeling the cells and the number of cells alive or dead post labeling under the different culture systems within which the probe was being studied.

The results from microscopy for the 2D hNPCs and neurons showed the cells were labeled starting at concentrations of 0.2mg/ml and 0.5mg/ml respectively **(Fig 6a &6b)**. Using flow cytometry, we showed that there were comparable number of live versus dead cells in the labeled versus the unlabeled cells and an increase in the concentration of the probe did not cause cell death in either neurons or hNPCs **(Fig 6e&6f)**. At the single cell level for hNPCs using flow, we observed about 86% green fluorescence and a total of about 96% labeling at as low as 0.1mg/ml, at 0.1mg/ml there was low blue fluorescence **Fig 6c**. At 1mg/ml, the green and blue fluorescing cells was greater than 99%. We also observed about 99% of fluorescing neurons at 1mg/ml **Fig 6d**, in view of that, the optimal labeling concentration for the 2D system was finalized at 1mg/ml.

3.1.2 Microcarrier Labeling Efficiency

a.

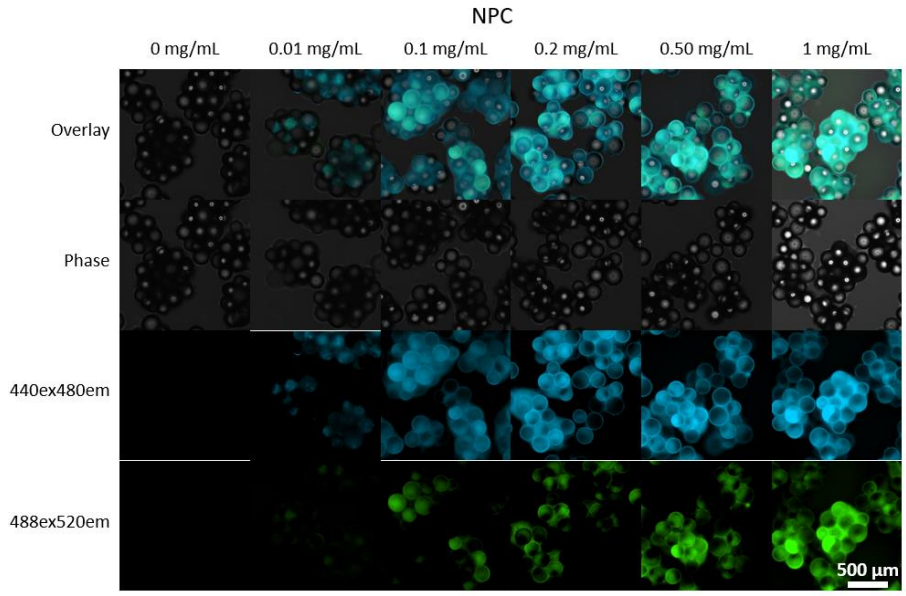

b.

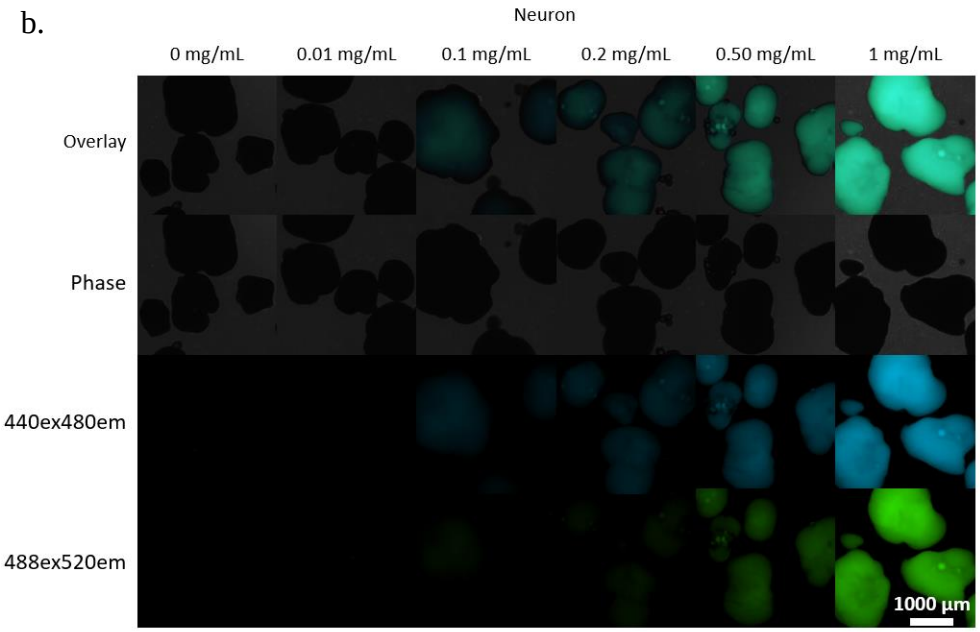

c.

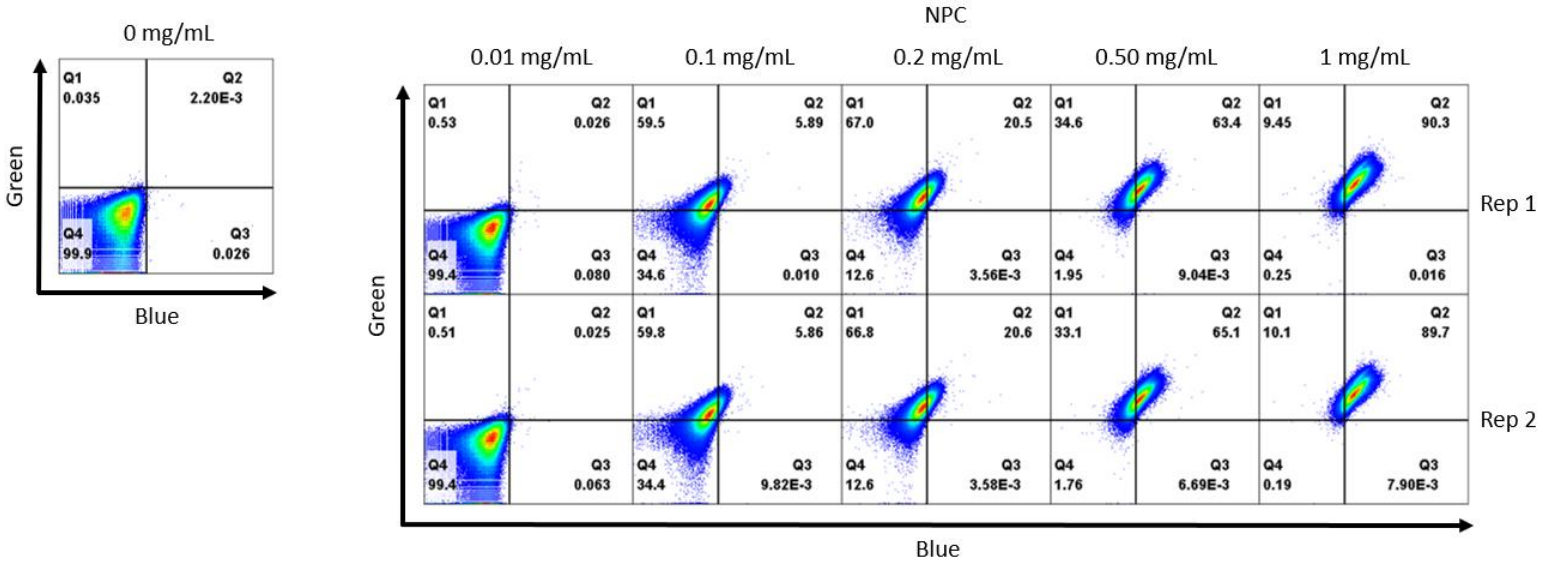
0 mg/mL
Q1 0.035
Q2 2.20E-3
Q4 99.9
Q3 0.026
Green
Blue
NPC
0.01 mg/mL
0.1 mg/mL
0.2 mg/mL
0.50 mg/mL
1 mg/mL
Q1 0.53
Q2 0.026
Q1 59.5
Q2 5.89
Q1 67.0
Q2 20.5
Q1 34.6
Q2 63.4
Q1 9.45
Q2 90.3
Q4 99.4
Q3 0.080
Q4 34.6
Q3 0.010
Q4 12.6
Q3 3.56E-3
Q4 1.95
Q3 9.04E-3
Q4 0.25
Q3 0.016
Rep 1
Q1 0.51
Q2 0.025
Q1 59.8
Q2 5.86
Q1 66.8
Q2 20.6
Q1 33.1
Q2 65.1
Q1 10.1
Q2 89.7
Q4 99.4
Q3 0.063
Q4 34.4
Q3 9.82E-3
Q4 12.6
Q3 3.58E-3
Q4 1.76
Q3 6.69E-3
Q4 0.19
Q3 7.90E-3
Rep 2
Green
Blue

d.

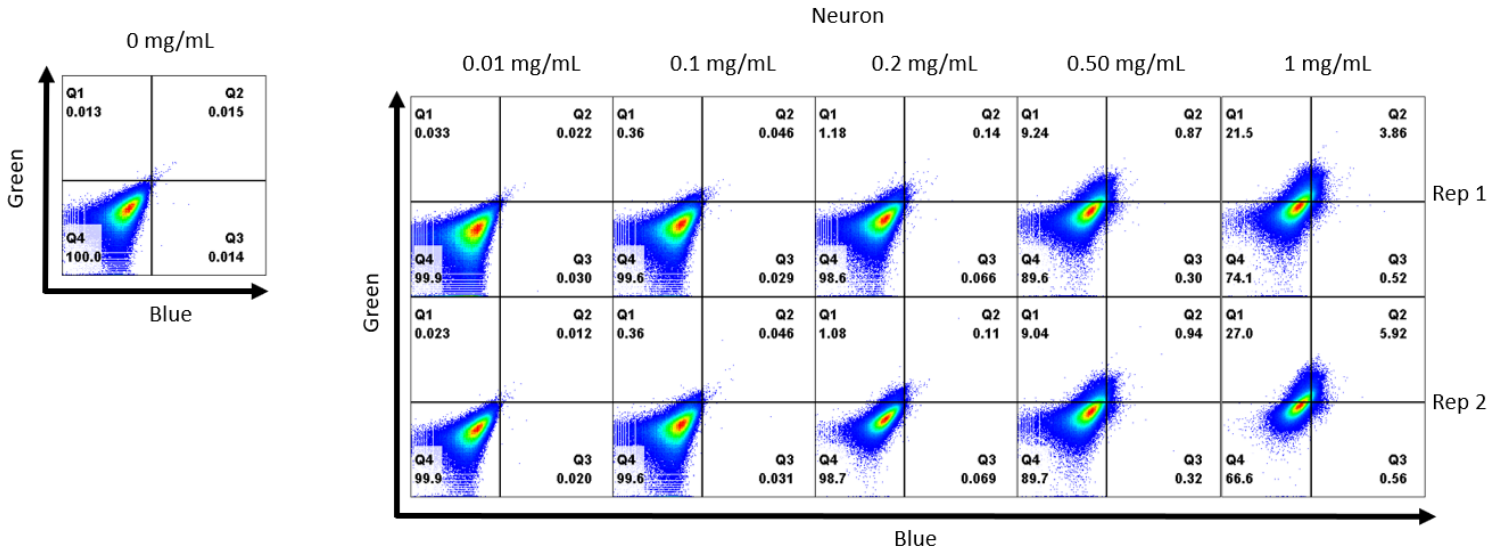
0 mg/mL
Q1 0.013
Q2 0.015
Q4 100.0
Q3 0.014
Green
Blue
Neuron
0.01 mg/mL
0.1 mg/mL
0.2 mg/mL
0.50 mg/mL
1 mg/mL
Q1 0.033
Q2 0.022
Q1 0.36
Q2 0.046
Q1 1.18
Q2 0.14
Q1 9.24
Q2 0.87
Q1 21.5
Q2 3.86
Q4 99.9
Q3 0.030
Q4 99.6
Q3 0.029
Q4 98.6
Q3 0.066
Q4 89.6
Q3 0.30
Q4 74.1
Q3 0.52
Rep 1
Q1 0.023
Q2 0.012
Q1 0.36
Q2 0.046
Q1 1.08
Q2 0.11
Q1 9.04
Q2 0.94
Q1 27.0
Q2 5.92
Q4 99.9
Q3 0.020
Q4 99.6
Q3 0.031
Q4 98.7
Q3 0.069
Q4 89.7
Q3 0.32
Q4 66.6
Q3 0.56
Rep 2
Green
Blue

e.

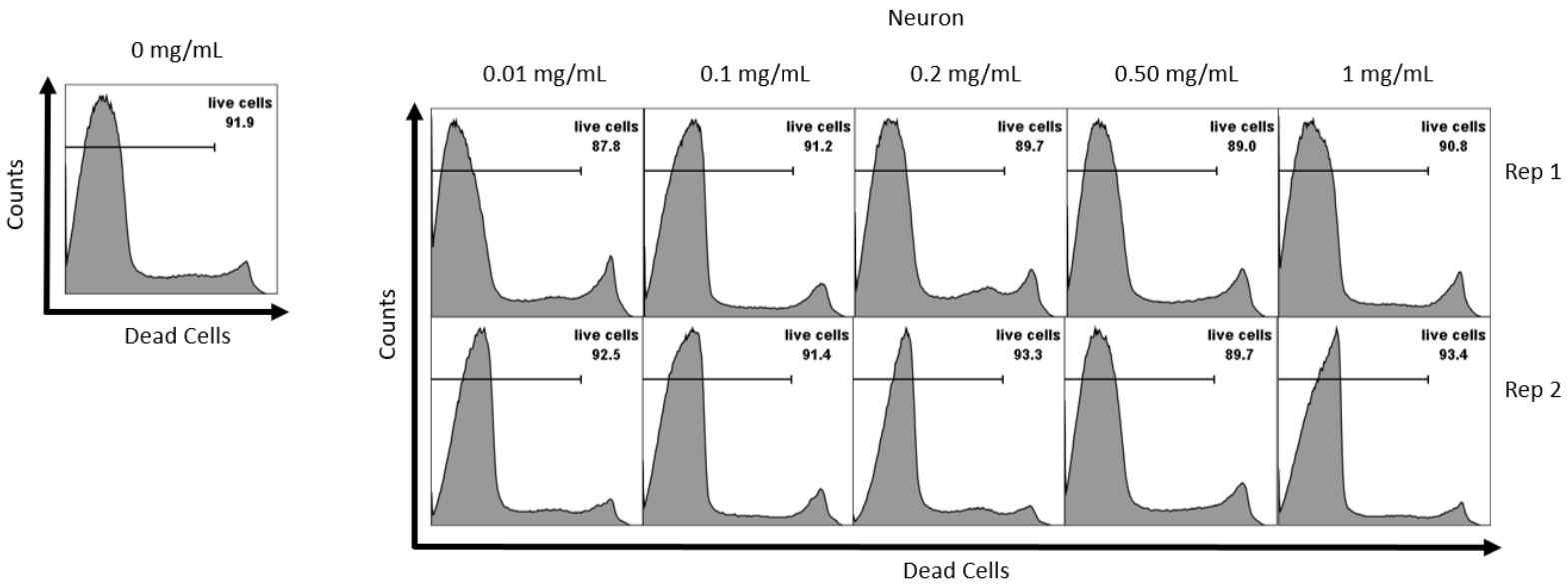

f.

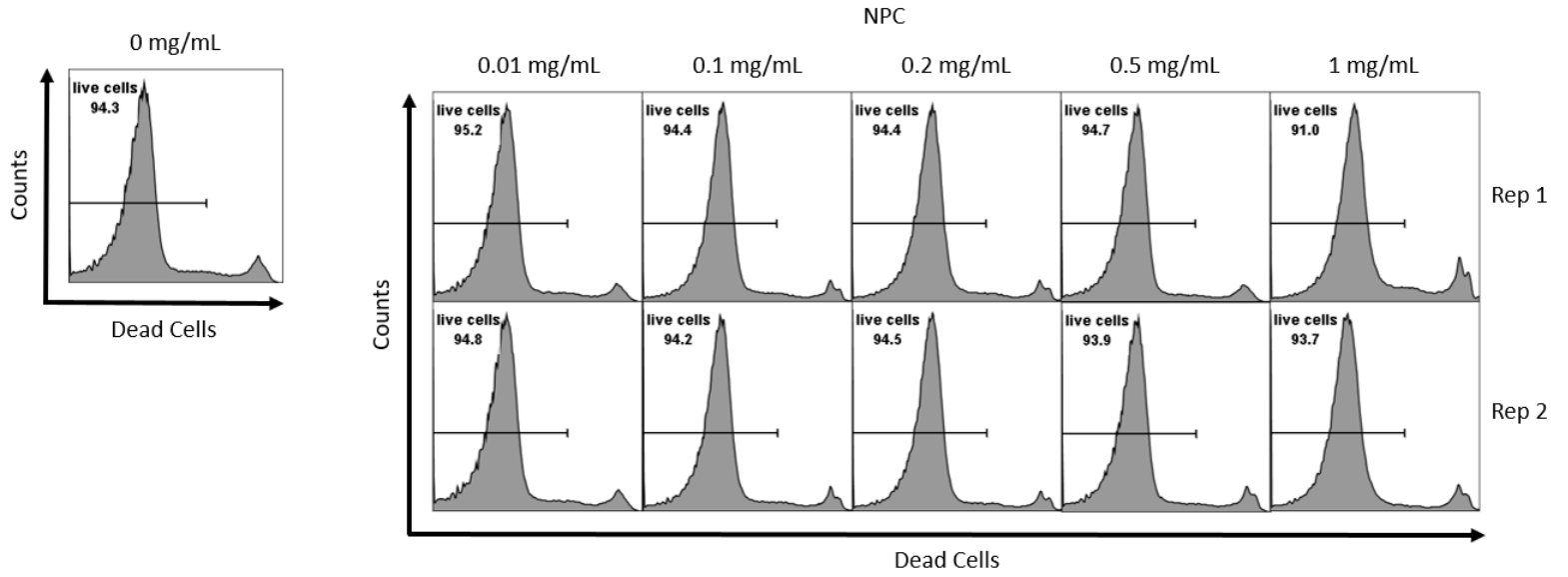

Figure 7: Microcarrier Labeling Efficiency: a & b) Fluorescent images of hNPCs and neurons respectively from a confocal microscope with excitations for blue and green emission for different concentration of the probe. c & d) Flow plot showing labeling with green and blue emissions for hNPCs and neurons respectively for different values of probe concentration. e & f) Histogram showing dead and live cells for hNPCs and neurons respectively at the different labeling concentration

In the microcarrier culture system, we observed onset of cell labeling using microscopy with concentration as low as 0.01 mg/ml in the hNPC group **Fig 7a** and about 0.2mg/ml in the neurons **Fig 7b.** The percentage of live/dead cells was observed to be comparable to the unlabeled cells with about 91% live cells at the optimal labeling concentration of 1mg/ml **(Fig 7e&7f)**. Live cells from the unlabeled group were used as the gate to compare with the labeled cells at the different concentration of the pH probe. At the optimal labeling concentration, we observed about 97% cell labeling in hNPCs **Fig 7c** but not in the neurons. The neurons showed about 34% labeling **Fig 7d,** which we believe is associated with the long protocol required to dissociate the neurons from the MCs into single cells prior to flow cytometry rather than an issue of the probe.

3.1.3 Matrigel Labeling Efficiency

a.

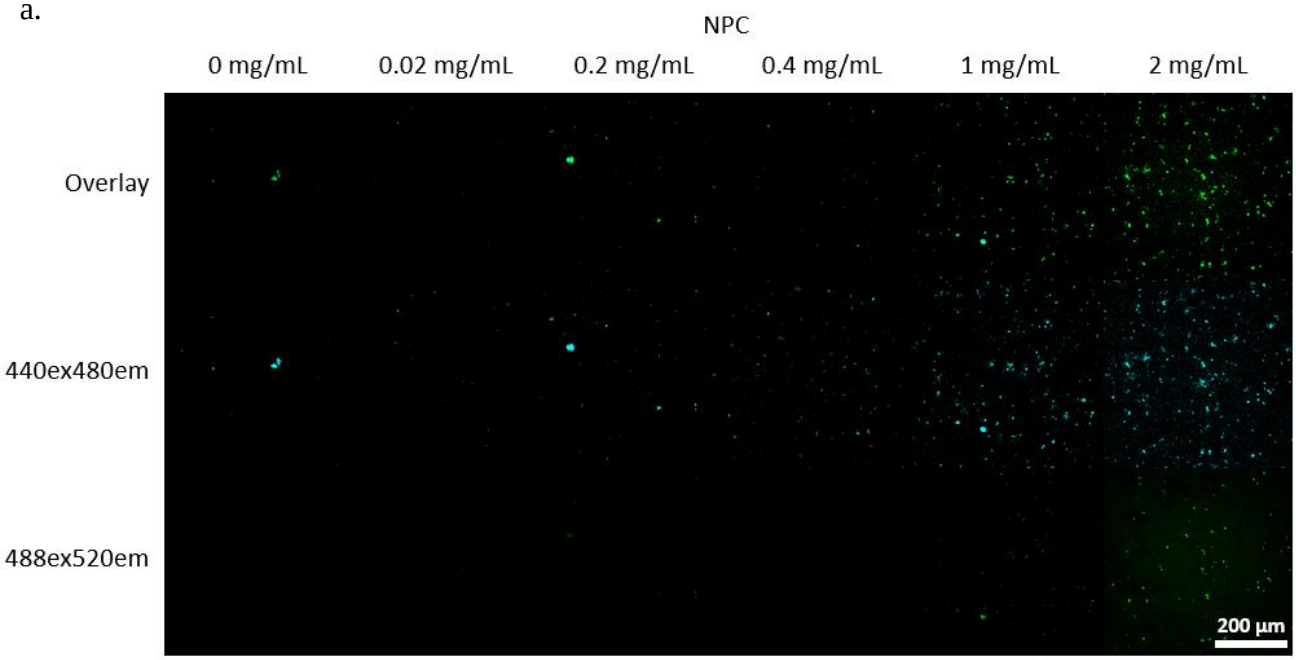

b.

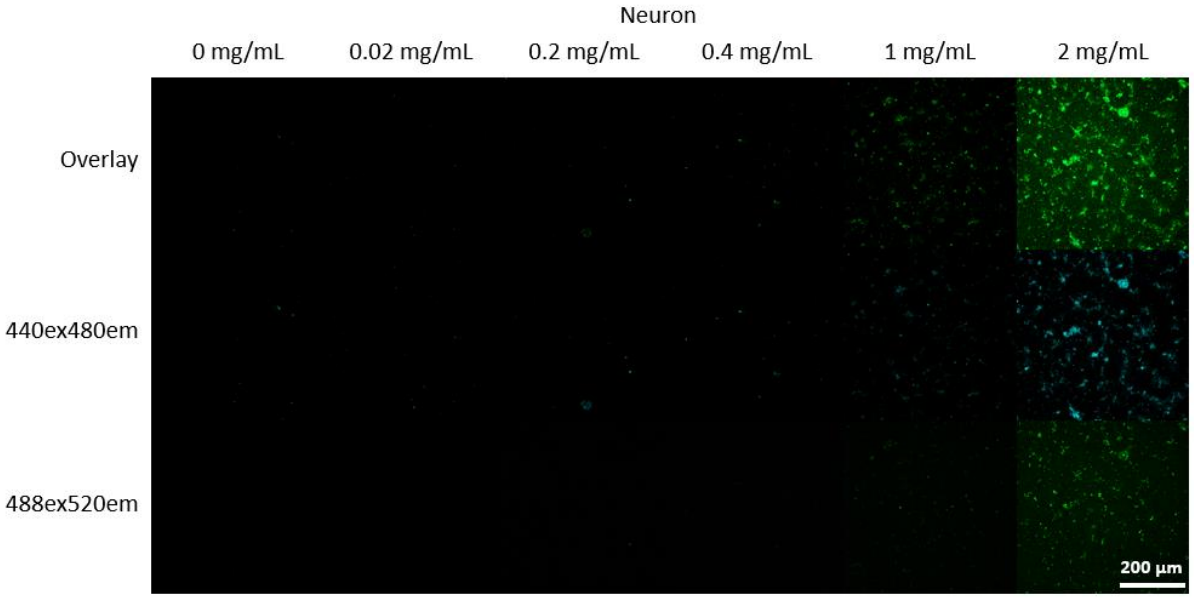

c.

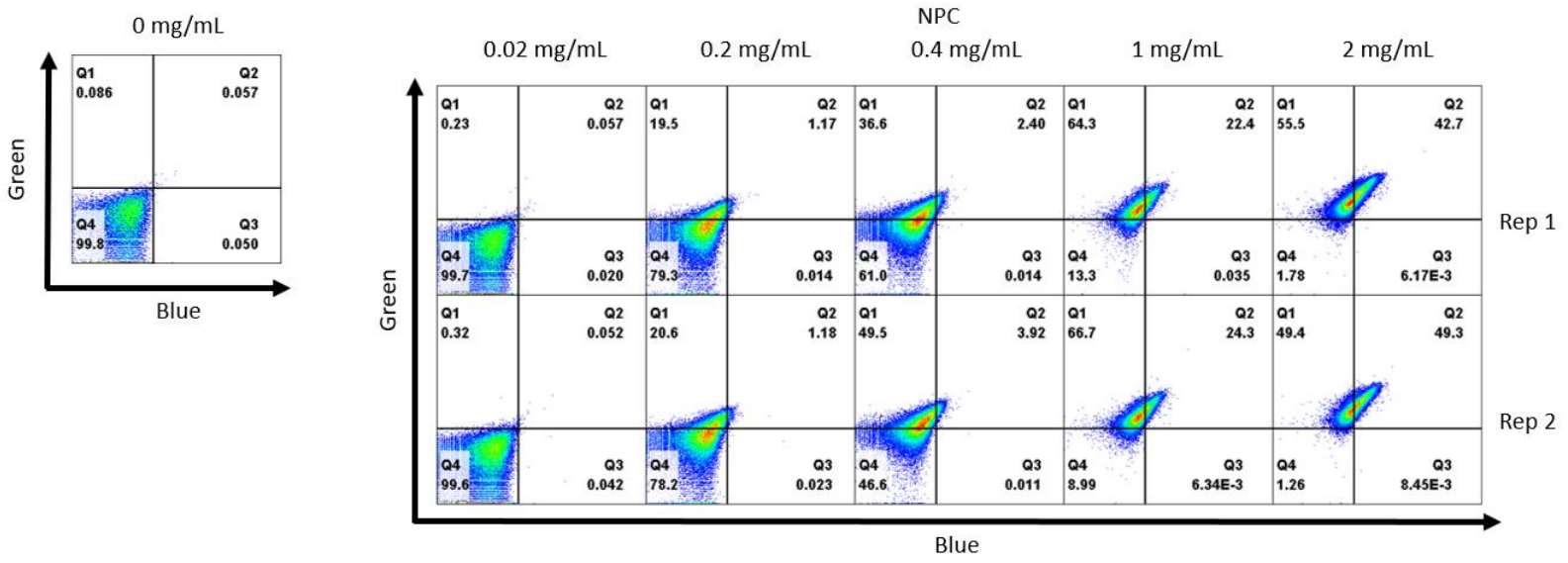
0 mg/mL
Q1 0.086
Q2 0.057
Q4 99.8
Q3 0.050
Green
Blue
NPC
0.02 mg/mL
0.2 mg/mL
0.4 mg/mL
1 mg/mL
2 mg/mL
Q1 0.23
Q2 0.057
Q4 99.7
Q3 0.020
Q1 19.5
Q2 1.17
Q4 79.3
Q3 0.014
Q1 36.6
Q2 2.40
Q4 61.0
Q3 0.014
Q1 64.3
Q2 22.4
Q4 13.3
Q3 0.035
Q1 55.5
Q2 42.7
Q4 1.78
Q3 6.17E-3
Rep 1
Q1 0.32
Q2 0.052
Q4 99.6
Q3 0.042
Q1 20.6
Q2 1.18
Q4 78.2
Q3 0.023
Q1 49.5
Q2 3.92
Q4 46.6
Q3 0.011
Q1 66.7
Q2 24.3
Q4 8.99
Q3 6.34E-3
Q1 49.4
Q2 49.3
Q4 1.26
Q3 8.45E-3
Rep 2
Green
Blue

d.

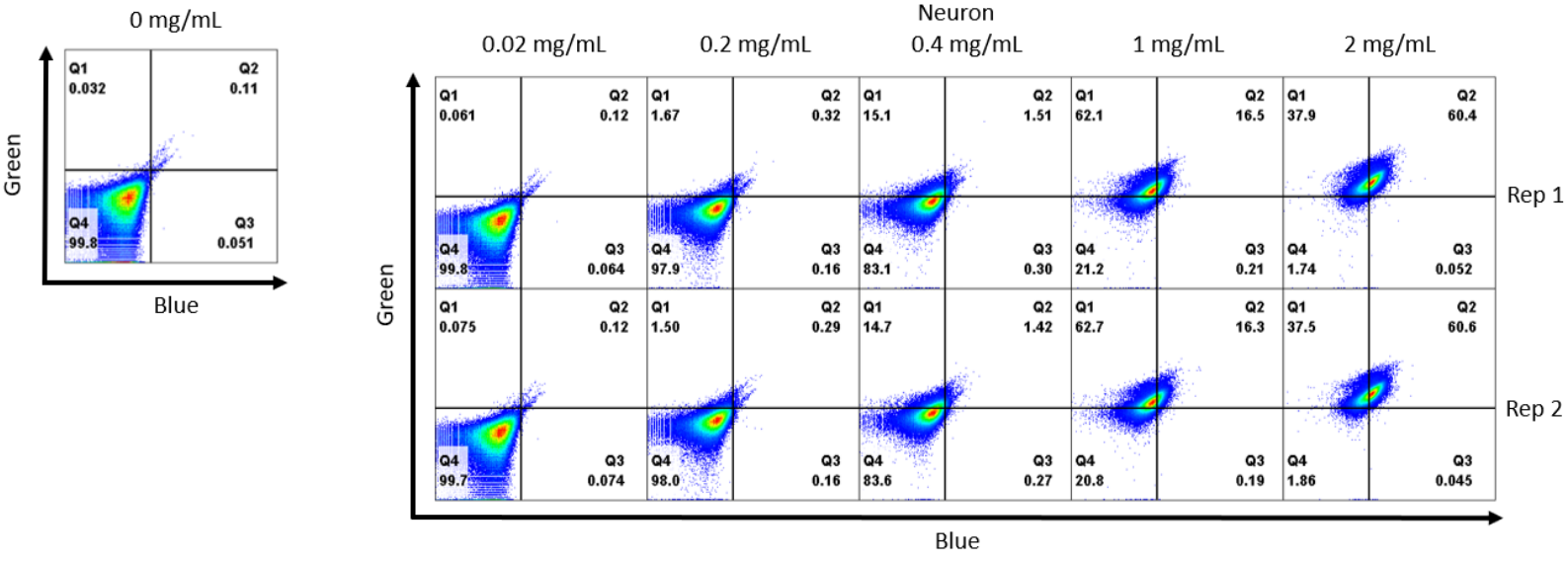
0 mg/mL
Q1 0.032
Q2 0.11
Q4 99.8
Q3 0.051
Green
Blue
Neuron
0.02 mg/mL
0.2 mg/mL
0.4 mg/mL
1 mg/mL
2 mg/mL
Q1 0.061
Q2 0.12
Q4 99.8
Q3 0.064
Q1 1.67
Q2 0.32
Q4 97.9
Q3 0.16
Q1 15.1
Q2 1.51
Q4 83.1
Q3 0.30
Q1 62.1
Q2 16.5
Q4 21.2
Q3 0.21
Q1 37.9
Q2 60.4
Q4 1.74
Q3 0.052
Rep 1
Q1 0.075
Q2 0.12
Q4 99.7
Q3 0.074
Q1 1.50
Q2 0.29
Q4 98.0
Q3 0.16
Q1 14.7
Q2 1.42
Q4 83.6
Q3 0.27
Q1 62.7
Q2 16.3
Q4 20.8
Q3 0.19
Q1 37.5
Q2 60.6
Q4 1.86
Q3 0.045
Rep 2
Green
Blue

e.

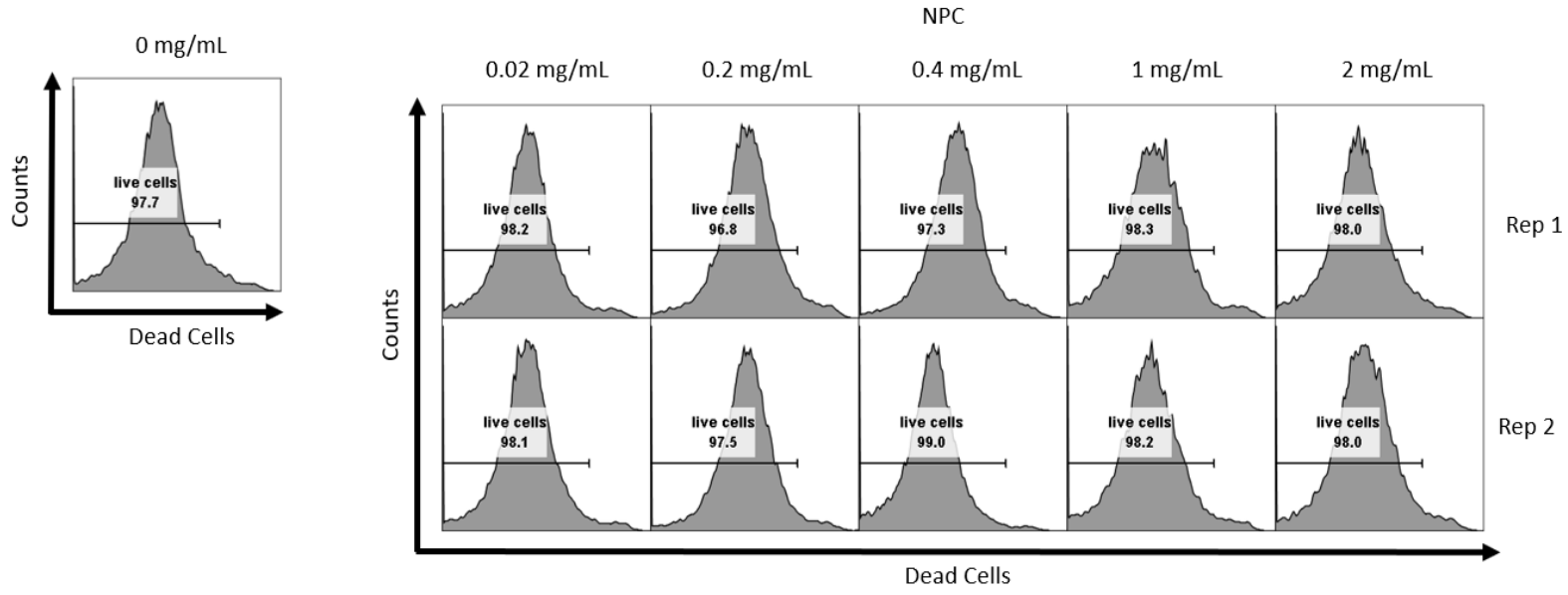

f.

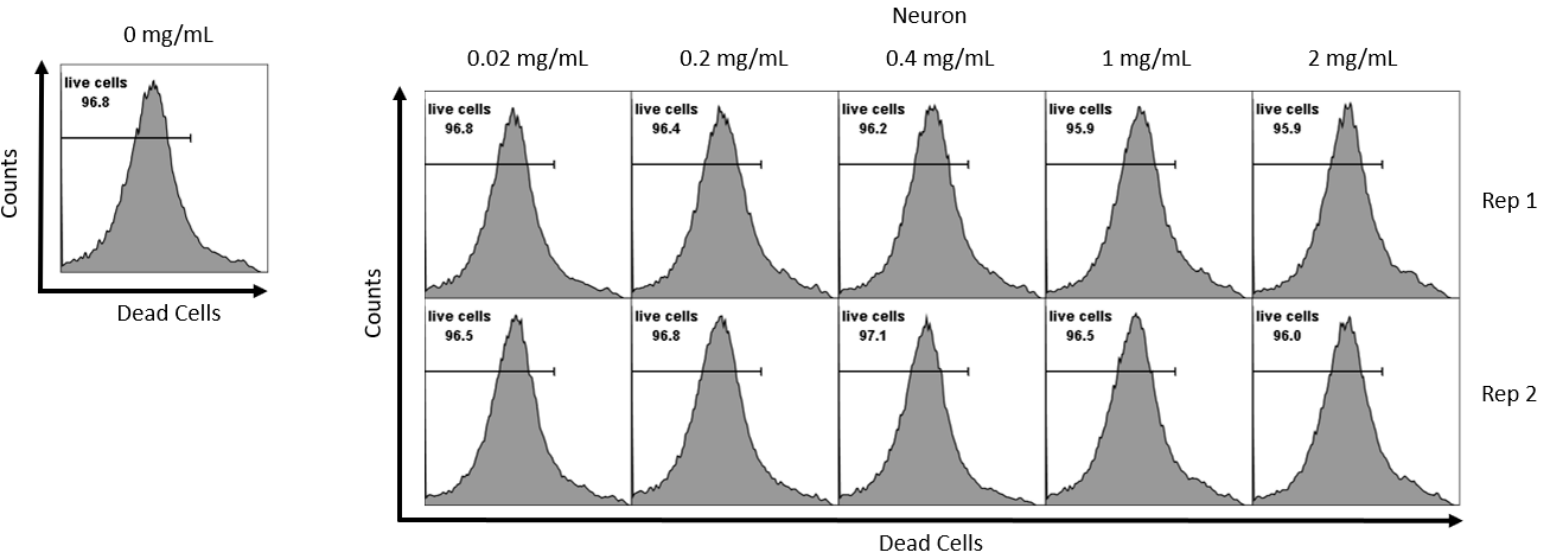

Figure 8: Matrigel Labeling Efficiency: a & b) Fluorescent images of hNPCs and neurons respectively from a confocal microscope with excitations for blue and green emission for different concentration of the probe. c & d) Flow plot showing labeling with green and blue emissions for hNPCs and neurons respectively for different values of probe concentration. e & f) Histogram showing dead and live cells for hNPCs and neurons respectively at the different labeling concentration

For hNPCs in Matrigel culture system, we observed onset of labeling using microscopy at concentration of 0.2mg/ml and observed neuron labeling at 1mg/ml **(Fig 8a&8b).** Similar to the other culture systems, the concentration of the pH did not initiate cell death and the percentage of live cells were about 98% and comparable to the unlabeled cells for both hNPCs and neurons **(Fig 8e&8f)**. The percentage labeled cells was less than 90% at a concentration of 1mg/ml in both hNPCs and neurons and about 98% for a concentration of 2mg/ml **(Fig 8c&8d)**. The optimum concentration for all experiments in the Matrigel culture system was then finalized at 2mg/ml.

Based on the results from all the culture systems, the pH probe showed early onset of labeling at low concentrations when the cells were considered individually using flow cytometry unlike that observed in the microscopy images. The above could be because the intensities quantitatively reported using flow cytometry is not visible to the naked eye and does not show in the microscopy images. In all the systems, the concentration of the probe did not initiate cell death, suggesting that the probe does not affect cell viability.

3.1.4 2D pH Dependency

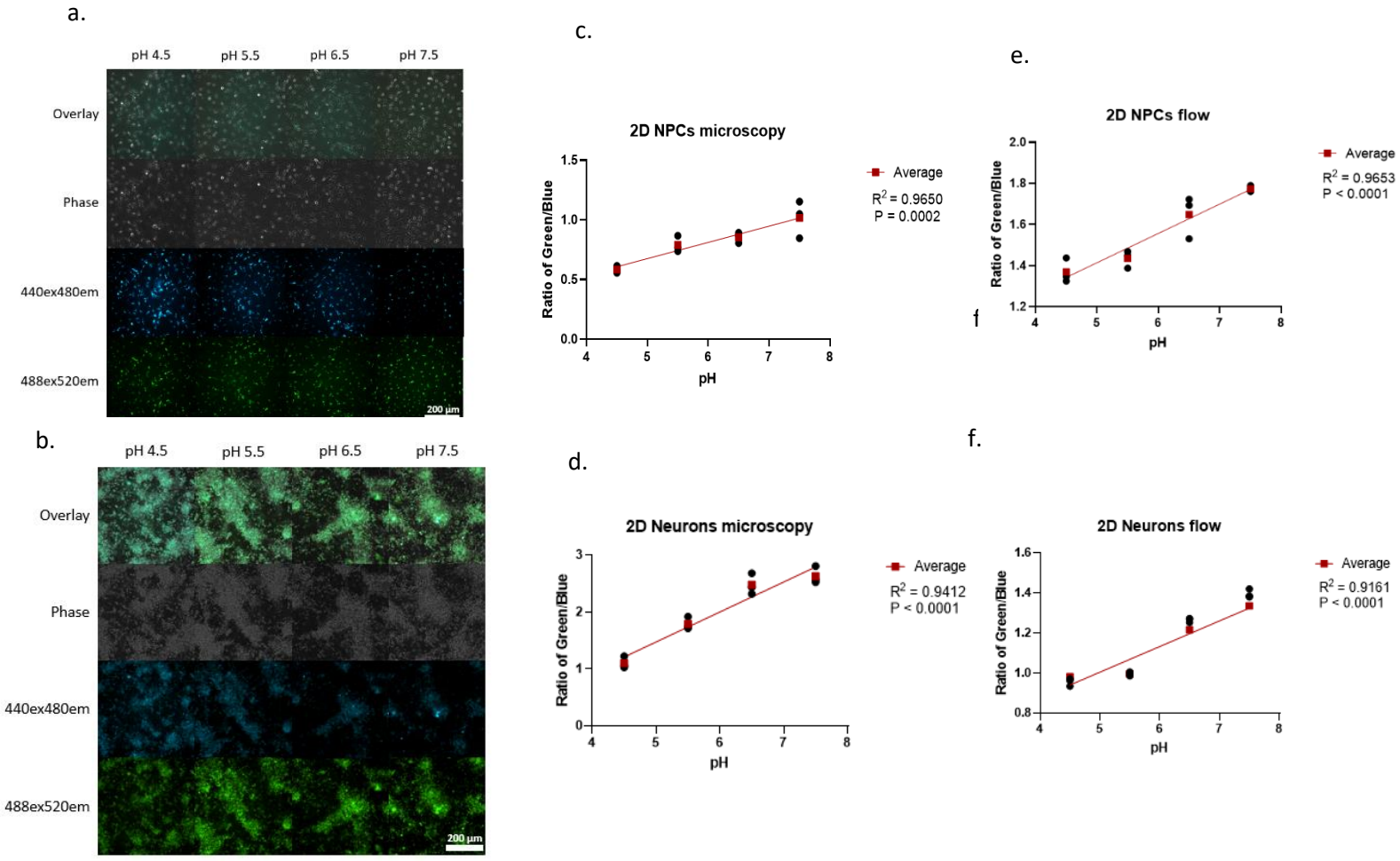

Figure 9: pH Dependency for 2D hNPC and 2D neurons, n=3 for all pH. a & b) Fluorescent images of hNPCs and neurons respectively from a confocal microscope with excitations for blue and green emission for different pH values. c) hNPC pH dependency plot with ratio of green on blue intensities verse pH using microscopy. d) Neuron pH dependency plot with ratio of green on blue intensities verse pH using microscopy. e) hNPC pH dependency plot with ratio of green on blue intensities verse pH using flow cytometry. f) Neuron pH dependency plot with ratio of green on blue intensities verse pH using flow cytometry

To test the pH dependency of the nanoprobes in 2D culture system, proliferating hNPCs and non-proliferating neuronal cells were cultured on 2D as describe in section 4.2.1 and 4.2.2. pH dependency was studied using both microscopy and flow cytometry for both cell types. pH buffers of the various pH for the test were added to the labeled cells prior to imaging or flow test, fluorescence images were taken **(Fig 9a&9b).** The ratiometric intensity (Green/blue) of the microscopy images were calculated using Matlab and the values were plotted against pH for both hNPCs and neurons (**Fig 9c&9d).** We observed a decreasing blue intensity and an increasing green intensity with increasing pH in the microscopy images as was previously reported by Su et al [17]. This was further confirmed by the results of intensity values from the images (**Fig 9c&9d)**. We used flow cytometry to study the intensity levels at single cell levels and for quantitative determination of the fluorescence and we observed significant changes in fluorescence with pH with great R-squared values in both neurons and hNPCs **(Fig 9e&9f).** This result confirmed the fluorescence pH dependency of the probe in 2D culture system in both proliferating and non-proliferating cells with ranges good enough to be visible to the naked eye and particularly prominent in neurons **Fig9b**.

3.1.5 Microcarrier pH Dependency

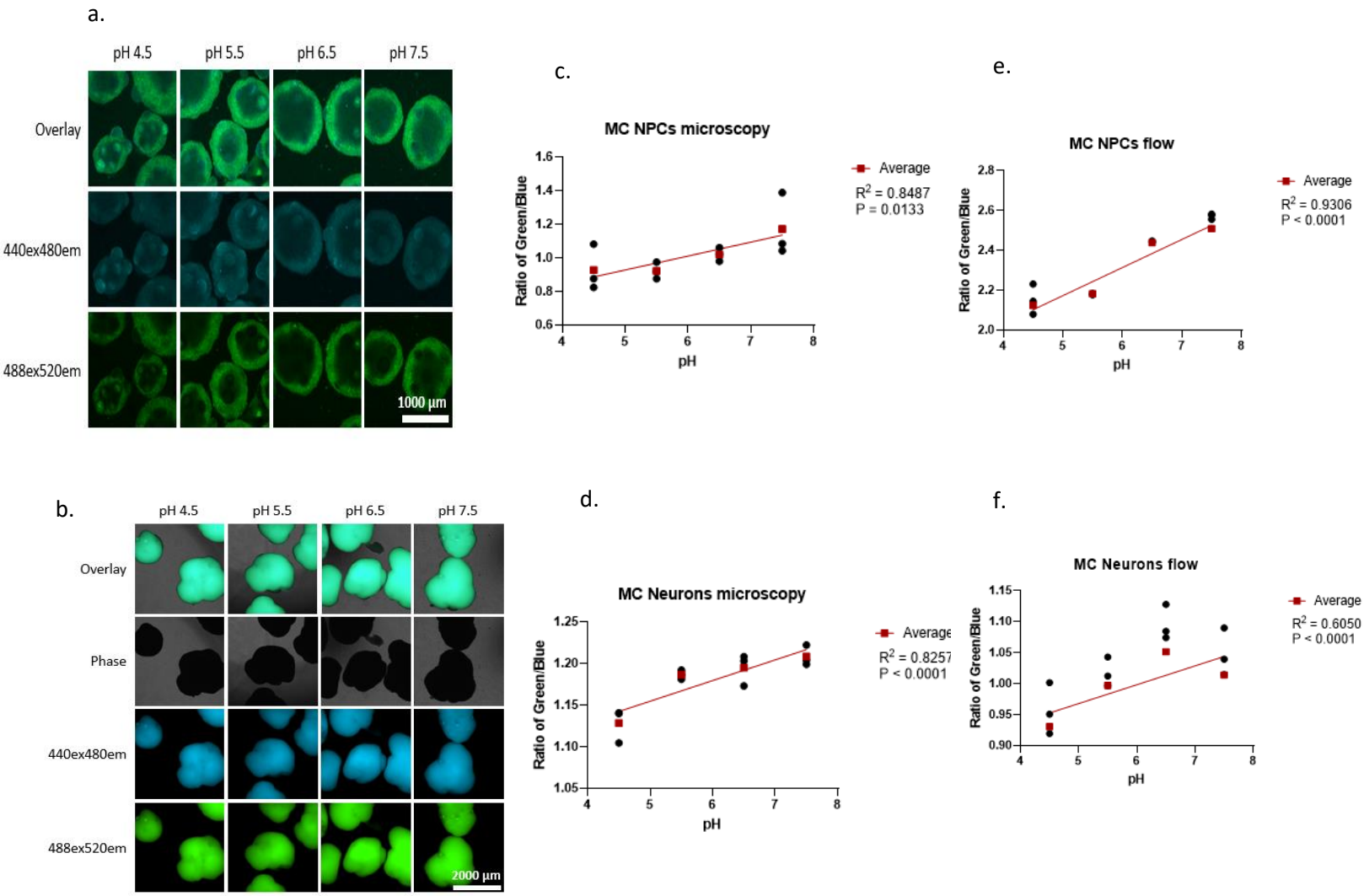

Figure 10:pH Dependency for Microcarrier hNPC and Neuron, n=3 for all pH. a & b) Fluorescent images of hNPCs and neurons respectively from a confocal microscope with excitations for blue and green emission for different pH values. c) hNPC pH dependency plot with ratio of green on blue intensities verse pH using microscopy. d) Neuron pH dependency plot with ratio of green on blue intensities verse pH using microscopy. e) hNPC pH dependency plot with ratio of green on blue intensities verse pH using flow cytometry f) Neuron pH dependency plot with ratio of green on blue intensities verse pH using flow cytometry

Cells were cultured on microcarriers as previously described in subsection 2.1.4 and 2.1.5. Images of the cells on microcarriers were taken for the fluorescence pH dependency and cells were dissociated from the microcarriers for single cell pH dependency using flow cytometry. Fluorescence images for both neurons and hNPCs did not show decreasing intensity in the blue channel with pH to the naked eye and no obvious increasing green fluorescence **Fig 10a &10b** relative to that which was observed in the 2D culture system. Despite the difficulty in observing the fluorescence changes with the eye, the intensity calculation showed a good correlation between pH and the ratiometric intensities green/blue **Fig 10c&10d**.

The range of the fluorescence intensities were observed to be lower than those in the 2D culture systems likewise the p-value and the R-squared values. Single cell pH dependency showed a better R-squared value in hNPCs compared to neurons with both showing significance in the pH changes with fluorescence **Fig 10e&10f**. The results demonstrated the capability of the pH sensitive probe to detect changes in pH in a microcarrier culture system and changing its fluorescence properties based on the detected pH changes.

3.1.6 Matrigel pH Dependency

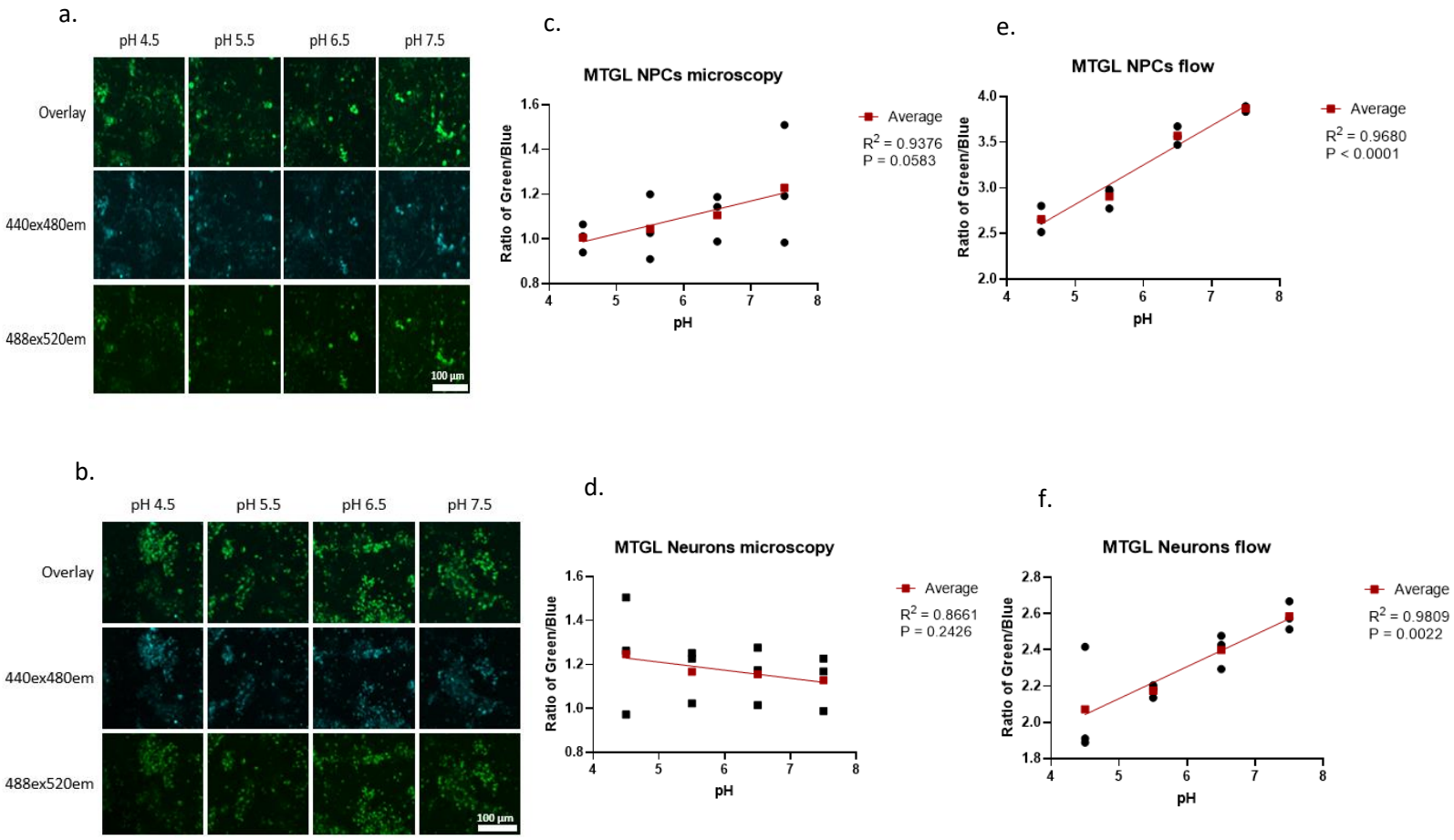

Figure 11: pH Dependency for 3D Matrigel hNPC and Neurons, n=3 for all pH. a & b) Fluorescent images of hNPCs and neurons respectively from a confocal microscope with excitations for blue and green emission for different pH values. c) hNPC pH dependency plot with ratio of green on blue intensities verse pH using microscopy. d) Neuron pH dependency plot with ratio of green on blue intensities verse pH using microscopy. e) hNPC pH dependency plot with ratio of green on blue intensities verse pH using flow cytometry. f) Neuron pH dependency plot with ratio of green on blue intensities verse pH using flow cytometry

Matrigel pH dependency was studied with both flow and microscopy as was done in other two culture systems. The results from the microscopy data were observed to be unreproducible in the neuronal culture system with an inverse relation different from our initial hypothesis and previous observations in other culture systems **Fig 11d**. The intensity calculations from the confocal images for both hNPCs neurons and did not show significance in p-value **(Fig 11c&11d)**. On the other hand, intensity measurement at the single cell level using flow cytometry showed good correlation with pH with statistical significance **(Fig 11e&11f)**. We observed gel depolymerization upon adding the pH buffer prior to imaging for the microscopy analysis and we believe the noncorrelation observed in the microscopy was because of imaging artifact presented by the depolymerized gel. We believe the depolymerization altered the actual fluorescence intensities from the probe and the imaging artifact was dependent on the degree of the depolymerized gel.

3.2 Cell Proliferation Studies

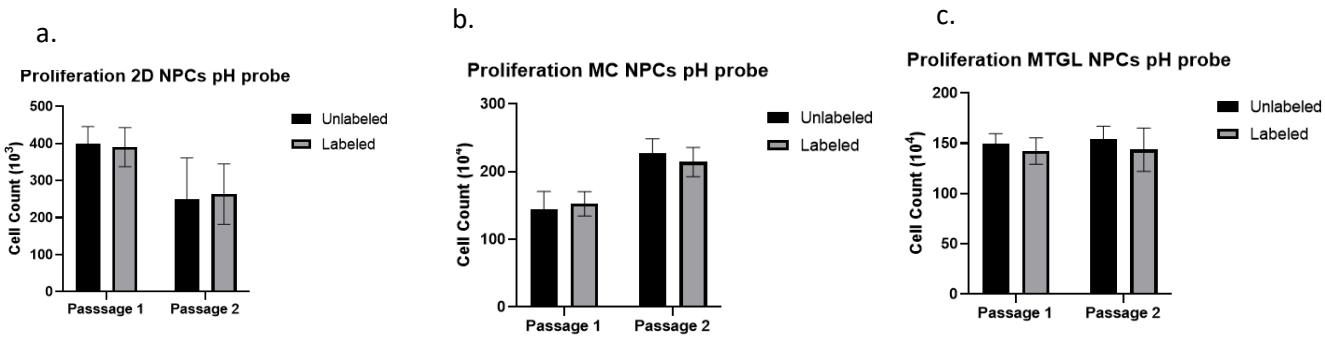

Figure 12: Cell Proliferation post labeling with ph probe. a) hNPC cell counts for two passages post labeling in 2D culture system. b) hNPC cell counts for two passages post labeling in MC culture system. c) hNPC cell counts for two separate triplicates each considered as a passage post labeling in Matrigel culture system.

The proliferation of stem cells has been reported to be supported by several polymers, some polymers support the self-renewal of stem cells in the short term while others can support the self-renewal of stem cells in the long term[30] [31]. Other studies have reported the reduction in stem cell proliferation in the application of polymers compared to non-polymer controls[32]. The pH sensing nanoprobe is a polymer based nanoprobe and therefore requires that we understand how it affects the self-renewal of proliferating cells.

In that regard, we studied the proliferation of human neural progenitor cells in the different culture systems when labeled with the nanoprobe and with an unlabeled control group. We seeded cells on 6 well plates coated with PLO and laminin prior to seeding and labeled the cells with the nanoprobe on day 1 post seeding. The probes were washed after 24hrs as required and cells were passaged and counted on day 3 at about 80% confluency and reseeded for a second

passage. Cells were not labeled on the second passage, we observed decrease in cell count between the first and the second passages without any significant change in cell count within passages between the unlabeled and the labeled cells in 2D **Fig 12a**. The decrease in cells count in the second passage compared to the first passage could be explained to be due to the later passage number as it has previously been reported that latter passages can significantly reduce stem cell proliferation[33].

In the microcarrier culture system, cells were seeded onto microcarriers, labeled on day 1 and passaged/dissociated on day 3. The cells were counted and reseeded onto microcarriers for the second passage and the cell count between labeled and unlabeled were compared **(Fig 12b)**. The increased number of cell count in the second passage was because it lasted longer (4 days) than the first passage (3 days) since the major concern was to study the differences between labeled and unlabeled cells within passages and not between passages.

The Matrigel system does not favor cells that much for passaging and reseeding and as a result, what is indicated above as passages is rather different sets of triplicates. We cultured cells on Matrigel and labeled them on day 1 post culture, washed after 24hrs and dissociated/passaged 48hrs post labeling. We observed decrease in cell count in the labeled cells compared to the unlabeled with no statistically significant differences between the two samples **(Fig 12c).** The above results demonstrate that the pH sensitive nanoprobe has no significant effects on the proliferative characteristics of hNPCs in all three different culture systems. For all the culture systems, the p-value from a two-way anova test was around 0.8 which showed there was no significant difference between the unlabeled and labeled cells with a passage.

3.3 Cell Specific Marker Expression (immunofluorescence)

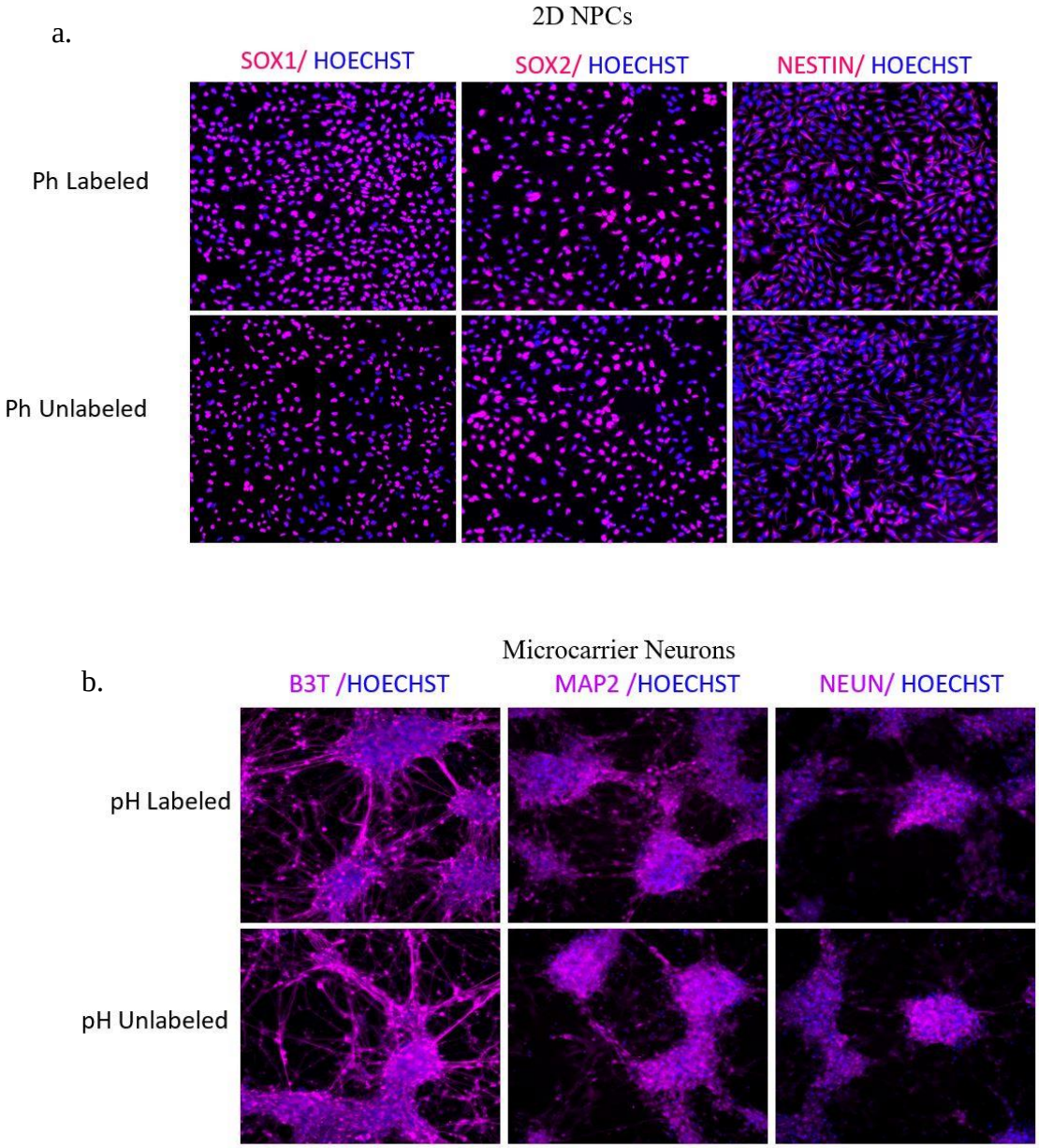

Figure 13: Immunofluorescence studies. a) Labeled and Unlabeled hNPCs expressing SOX1, SOX2 and NESTIN with DNA stained with HOECHST. b) Labeled and Unlabeled neurons expressing B3T, MAP2 and NEUN with DNA stained with HOECHST

To further investigate the effects of the probes on cell, we performed immunofluorescence studies to determine specific proteins to the cells we have been using in the experiment. We cultured cells and labeled them with the probe, we washed after 24 hours and allowed the cells to sit overnight. We fixed the cells, perm, and stain them with antibodies that binds to the proteins of interest to us. In our case, for hNPCs, we studied the expression of SOX1, SOX2 and NESTIN which are proteins expressed by neural progenitor cells. For the neurons, we investigated the expression of B3T, MAP2 and NEUN which are neuronal specific markers.

The results showed the expression of all the three markers studied for the hNPCs in both the labeled and unlabeled cells **Fig 13a**. The expression of the neuronal markers was also observed in both the labeled and unlabeled cells **Fig 13b.** We observed no obvious difference between the unlabeled and labeled group for any of the cell markers studied. The we stained the DNA with HOECHST, shown in blue in all images to confirm the presence of cells. These results qualitatively show that labeling with the pH probe does not affect the expression of cell specific markers and likewise its phenotype. Further, quantitative measurements of the expressions of these markers will be needed to validate conclusion.

DISCUSSION

Several intracellular pH monitoring probes have been developed. However, these technologies face multiple challenges spanning from bio-incompatibility, impermeability, inaccuracy, and many more[34]. Ratiometric analysis of pH has been demonstrated to provide a more accurate means of measurement independent of probe concentrations[35]. This led to the development of a ratiometric fluorescence and MRI based probe for intracellular pH monitoring[17]. This study examines the performance and phenotypical effects of the ratiometric probe using Hipsc derived neurons and NPCs.

We sought to investigate the optimum concentration of the probe for labeling of cells in all three experimental culture systems studied. Consistent with previous results, cells in 2D and microcarrier culture systems showed effective labeling at concentration of 1mg/ml. Cells in the matrigel culture system had a slight deviation with optimal labeling concentration of 2mg/ml, this could potentially be because of the 3D environment created by the culture system. We believe the 3D environment/ matrix structure hindered the transport of the probes to the cells and therefore required higher concentrations to label cells. Propidium iodide study confirms further that the viability of cells was not affected by probe labeling using unlabeled cells as control group. The observed lower viability of neurons compared to NPCs is accounted to the characteristic fragility of neurons and not due to the probe as was observed in the unlabeled neuron group as well.

We also sought to investigate the fluorescence pH dependence of the probe in all three culture systems. The probe demonstrated ratiometric fluorescence-based pH dependencies using

confocal microscopy in the 2D and microcarrier culture systems but not in Matrigel. The uncorrelated pH dependency observed in the Matrigel culture using microscopy was likely associated with the depolymerization of the gel observed upon addition and subsequent incubation with the pH buffer. The gel depolymerization could potentially introduce imaging artifacts that could potentially alter the actual intensities received from the probe. This could be further confirmed by the pH dependency results determined using flow cytometry; all culture systems including Matrigel demonstrated pH dependency using the flow cytometry method. Gel depolymerization is not observed in the flow cytometry method because cells were dissociated from the Matrigel before the addition of the pH buffer. It should be noted that the flow cytometry method requires cell dissociation which cannot when the cells are needed for further experiment as the sterility and the treatment process will not allow cell re-usage. The microscopy technique on the other hand, can be used when the cells are needed for further experiment as most imaging systems have sterile environment and the process of imaging might not affect the cells.

Through further studies of neuronal and NPC markers, it was observed that SOX1, SOX2 and NESTIN were equally expressed qualitatively by both unlabeled NPCs and labeled NPCs. The expression of B3T, MAP2 and NEUN was also confirmed post labeling with the probe. These results present the idea that neuronal and NPC phenotypes of the cells were not affected by labeling with the pH probe by qualitative observation of the fluorescent images of these markers. Further quantitative methods for determining the expression of these cell specific markers using quantitative PCR is ongoing and will help to finalize whether or not there is any significant differences in the expression of these markers between the unlabeled and labeled cells.

All in all, these findings indicate that the ratiometric pH probe effectively labels cells in 2D, microcarrier and 3D Matrigel culture systems while demonstrating ratiometric fluorescence pH dependency without affecting cell viability or cell phenotype.

4 CONCLUSIONS

The large scale biomanufacturing of cells and tissues present the potential for improved disease modeling, drug screening and cell-based drug development for the numerous uncurable diseases. Despite the promise and potentials of the biomanufacturing industry, batch to batch variability resulting mainly from constant in-line monitoring has being a cancer to the industry. Current pH probes for in-line monitoring of cells have faced several problems which resulted in the development of a new pH probe utilizing advanced monitoring modality for pH monitoring.

In this study, the performance and phenotypical effects of the advanced pH probe was investigated using hipsc derived neurons and NPCs under practical and commercially applicable cell culture systems. Our results demonstrated pH dependency in all culture conditions and further confirmed that the viability of cells is not affected by labeling with the pH probe. The reproducible pH dependency results using both microscopy and flow cytometry further confirms the adaptability of the probe for use in a standard biomanufacturing process with availability of either flow cytometer or a confocal microscopy. Staining for neuronal and NPC specific markers affirmed that cellular phenotype is not affected by labeling with the probe.

Altogether, our results indicate that the ratiometric pH probe capable of labeling cells in different culture systems and exhibits fluorescence-based pH dependency without impacting cell viability and phenotype. Our results supported the adaptability of the probe as it could be used where either a flow cytometer or a confocal microscope is available.

5 FUTURE WORK

In this study, we investigated labeling efficiency, cell viability, pH dependency and phenotypic effects of the pH probe under different culture conditions using proliferating and non-proliferating cells. To further demonstrate accuracy of the pH probe, it should be studied under a more specific previously studied system while comparing the results. To that effect, the probe could be investigated in differentiating cells to understand its accuracy in distinguishing between differentiating and non-differentiating cells, as cell differentiation has been reported to be pH dependent

REFERENCES:

[1] "Pluripotent stem cells in disease modelling and drug discovery | Nature Reviews Molecular Cell Biology." https://www.nature.com/articles/nrm.2015.27 (accessed Mar. 13, 2021).

[2] R. Eiges *et al.*, "Developmental Study of Fragile X Syndrome Using Human Embryonic Stem Cells Derived from Preimplantation Genetically Diagnosed Embryos," *Cell Stem Cell*, vol. 1, no. 5, pp. 568–577, Nov. 2007, doi: 10.1016/j.stem.2007.09.001.

[3] K. J. Brennand *et al.*, "Modelling schizophrenia using human induced pluripotent stem cells," *Nature*, vol. 473, no. 7346, Art. no. 7346, May 2011, doi: 10.1038/nature09915.

[4] B. A. DeRosa *et al.*, "Derivation of autism spectrum disorder-specific induced pluripotent stem cells from peripheral blood mononuclear cells," *Neurosci. Lett.*, vol. 516, no. 1, pp. 9–14, May 2012, doi: 10.1016/j.neulet.2012.02.086.

[5] S.-Y. Ng *et al.*, "Genome-wide RNA-Seq of Human Motor Neurons Implicates Selective ER Stress Activation in Spinal Muscular Atrophy," *Cell Stem Cell*, vol. 17, no. 5, pp. 569–584, Nov. 2015, doi: 10.1016/j.stem.2015.08.003.

[6] G. Lee *et al.*, "Large-scale screening using familial dysautonomia induced pluripotent stem cells identifies compounds that rescue IKBKAP expression," *Nat. Biotechnol.*, vol. 30, no. 12, Art. no. 12, Dec. 2012, doi: 10.1038/nbt.2435.

[7] G. Lee *et al.*, "Modelling pathogenesis and treatment of familial dysautonomia using patient-specific iPSCs," *Nature*, vol. 461, no. 7262, pp. 402–406, Sep. 2009, doi: 10.1038/nature08320.

[8] D. Sareen, A. D. Ebert, B. M. Heins, J. V. McGivern, L. Ornelas, and C. N. Svendsen, "Inhibition of apoptosis blocks human motor neuron cell death in a stem cell model of spinal muscular atrophy," *PloS One*, vol. 7, no. 6, p. e39113, 2012, doi: 10.1371/journal.pone.0039113.

[9] J. L. Gordon, M. A. Brown, and M. M. Reynolds, "Cell-Based Methods for Determination of Efficacy for Candidate Therapeutics in the Clinical Management of Cancer," *Diseases*, vol. 6, no. 4, Sep. 2018, doi: 10.3390/diseases6040085.

[10] A. Ishaque and M. Al-Rubeai, "Use of intracellular pH and annexin-V flow cytometric assays to monitor apoptosis and its suppression by bcl-2 over-expression in hybridoma cell culture," *J. Immunol. Methods*, vol. 221, no. 1, pp. 43–57, Dec. 1998, doi: 10.1016/S0022-1759(98)00166-5.

[11] R. A. Gottlieb, "Cell acidification in apoptosis," *Apoptosis*, vol. 1, no. 1, pp. 40–48, Aug. 1996, doi: 10.1007/BF00142077.

[12] X. Zhang, Y. Lin, and R. J. Gillies, "Tumor pH and Its Measurement," *J. Nucl. Med.*, vol. 51, no. 8, pp. 1167–1170, Aug. 2010, doi: 10.2967/jnumed.109.068981.

[13] J. R. Casey, S. Grinstein, and J. Orlowski, "Sensors and regulators of intracellular pH," *Nat. Rev. Mol. Cell Biol.*, vol. 11, no. 1, Art. no. 1, Jan. 2010, doi: 10.1038/nrm2820.

[14] S. Sinharay and M. D. Pagel, "Advances in Magnetic Resonance Imaging Contrast Agents for Biomarker Detection," *Annu. Rev. Anal. Chem.*, vol. 9, no. 1, pp. 95–115, Jun. 2016, doi: 10.1146/annurev-anchem-071015-041514.

[15] B. Short, "A basic guide to stem cell differentiation," *J. Cell Biol.*, vol. 215, no. 3, pp. 293–293, Nov. 2016, doi: 10.1083/jcb.2153if.

[16] S. Tatapudy, F. Aloisio, D. Barber, and T. Nystul, “Cell fate decisions: emerging roles for metabolic signals and cell morphology,” *EMBO Rep.*, vol. 18, no. 12, pp. 2105–2118, Dec. 2017, doi: 10.15252/embr.201744816.
[17] F. Su *et al.*, “Multifunctional PHPMA-Derived Polymer for Ratiometric pH Sensing, Fluorescence Imaging, and Magnetic Resonance Imaging,” *ACS Appl. Mater. Interfaces*, vol. 10, no. 2, pp. 1556–1565, Jan. 2018, doi: 10.1021/acsami.7b15796.
[18] W. Zhang *et al.*, “A highly sensitive acidic pH fluorescent probe and its application to HepG2 cells,” *Analyst*, vol. 134, no. 2, pp. 367–371, Feb. 2009, doi: 10.1039/B807581F.
[19] C. Marini *et al.*, “A PET/CT approach to spinal cord metabolism in amyotrophic lateral sclerosis,” *Eur. J. Nucl. Med. Mol. Imaging*, vol. 43, no. 11, pp. 2061–2071, Oct. 2016, doi: 10.1007/s00259-016-3440-3.
[20] J. H. Jung, Y. Choi, and K. C. Im, “PET/MRI: Technical Challenges and Recent Advances,” *Nucl. Med. Mol. Imaging*, vol. 50, no. 1, pp. 3–12, Mar. 2016, doi: 10.1007/s13139-016-0393-1.
[21] “Simultaneous fluorescence and positron emission tomography for in vivo imaging of small animals.” https://www.spiedigitallibrary.org/journals/journal-of-biomedical-optics/volume-16/issue-12/120511/Simultaneous-fluorescence-and-positron-emission-tomography-for-in-vivo-imaging/10.1117/1.3665438.full (accessed Mar. 25, 2021).
[22] L. Q. Chen and M. D. Pagel, “Evaluating pH in the Extracellular Tumor Microenvironment Using CEST MRI and Other Imaging Methods,” *Adv. Radiol.*, vol. 2015, p. e206405, Jul. 2015, doi: 10.1155/2015/206405.
[23] Y. Kurishita, T. Kohira, A. Ojida, and I. Hamachi, “Rational design of FRET-based ratiometric chemosensors for in vitro and in cell fluorescence analyses of nucleoside polyphosphates,” *J. Am. Chem. Soc.*, vol. 132, no. 38, pp. 13290–13299, Sep. 2010, doi: 10.1021/ja103615z.
[24] W. Shi, X. Li, and H. Ma, “Fluorescent probes and nanoparticles for intracellular sensing of pH values,” *Methods Appl. Fluoresc.*, vol. 2, no. 4, p. 042001, Dec. 2014, doi: 10.1088/2050-6120/2/4/042001.
[25] J. Zhou, C. Fang, T. Chang, X. Liu, and D. Shangguan, “A pH sensitive ratiometric fluorophore and its application for monitoring the intracellular and extracellular pHs simultaneously,” *J. Mater. Chem. B*, vol. 1, no. 5, pp. 661–667, Jan. 2013, doi: 10.1039/C2TB00179A.
[26] H. Lu *et al.*, “A series of poly[N-(2-hydroxypropyl)methacrylamide] copolymers with anthracene-derived fluorophores showing aggregation-induced emission properties for bioimaging,” *J. Polym. Sci. Part Polym. Chem.*, vol. 50, no. 5, pp. 890–899, Mar. 2012, doi: 10.1002/pola.25841.
[27] H. Lu *et al.*, “Using fluorine-containing amphiphilic random copolymers to manipulate the quantum yields of aggregation-induced emission fluorophores in aqueous solutions and the use of these polymers for fluorescent bioimaging,” *J. Mater. Chem.*, vol. 22, no. 19, pp. 9890–9900, May 2012, doi: 10.1039/C2JM30258F.
[28] F. A. Rojas-Quijano *et al.*, “Synthesis and Characterization of a Hypoxia-Sensitive MRI Probe,” *Chem. Weinh. Bergstr. Ger.*, vol. 18, no. 31, pp. 9669–9676, Jul. 2012, doi: 10.1002/chem.201200266.
[29] “Papain Dissociation System - Worthington Enzyme Manual.” http://www.worthington-biochem.com/PDS/ (accessed Mar. 07, 2021).

[30] D. A. Brafman, C. W. Chang, A. Fernandez, K. Willert, S. Varghese, and S. Chien, "Long-term human pluripotent stem cell self-renewal on synthetic polymer surfaces," *Biomaterials*, vol. 31, no. 34, pp. 9135–9144, Dec. 2010, doi: 10.1016/j.biomaterials.2010.08.007.
[31] S. Pernagallo, J. Jose Diaz-Mochon, and M. Bradley, "A cooperative polymer-DNA microarray approach to biomaterial investigation," *Lab. Chip*, vol. 9, no. 3, pp. 397–403, 2009, doi: 10.1039/B808363K.
[32] P. Černochová *et al.*, "Cell type specific adhesion to surfaces functionalised by amine plasma polymers," *Sci. Rep.*, vol. 10, no. 1, Art. no. 1, Jun. 2020, doi: 10.1038/s41598-020-65889-y.
[33] Y. Gu *et al.*, "Changes in mesenchymal stem cells following long-term culture in vitro," *Mol. Med. Rep.*, vol. 13, no. 6, pp. 5207–5215, Jun. 2016, doi: 10.3892/mmr.2016.5169.
[34] W. Shi, X. Li, and H. Ma, "Fluorescent probes and nanoparticles for intracellular sensing of pH values," *Methods Appl. Fluoresc.*, vol. 2, no. 4, p. 042001, Dec. 2014, doi: 10.1088/2050-6120/2/4/042001.
[35] "Rational Design of FRET-Based Ratiometric Chemosensors for in Vitro and in Cell Fluorescence Analyses of Nucleoside Polyphosphates | Journal of the American Chemical Society." https://pubs.acs.org/doi/10.1021/ja103615z (accessed Apr. 12, 2021).